DEVELOPMENT OF SMA ACTUATED THREE-LINK ARM

by
SANJAY DUREJA

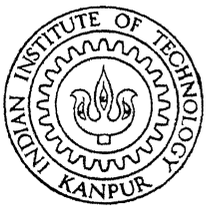

DEPARTMENT OF MECHANICAL ENGINEERING
INDIAN INSTITUTE OF TECHNOLOGY KANPUR

MARCH, 1990

DEVELOPMENT OF SMA ACTUATED THREE-LINK ARM

A Thesis Submitted
in Partial Fulfilment of the Requirements
for the Degree of
MASTER OF TECHNOLOGY

by

SANJAY DUREJA

to the

DEPARTMENT OF MECHANICAL ENGINEERING
INDIAN INSTITUTE OF TECHNOLOGY KANPUR

MARCH, 1990

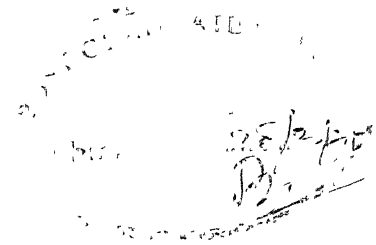

CERTIFICATE

This is to certify that the present work on "DEVELOPMENT OF SMA ACTUATED THREE - LINK ARM " by SANJAY DUREJA, has been carried out under our supervision and has not been submitted elsewhere for award of a degree.

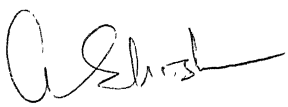

(Amitabha Ghosh)
Professor and Head
Mechanical Engineering
I.I.T Kanpur

(H.Hatwal)
Assistant Professor
Mechanical Engineering
I.I.T. Kanpur

March,1990.

Dedicated to

my Parents

and Brother

ACKNOWLEDGEMENT

I am deeply grateful to Dr. A. Ghosh and Dr. H. Hatwal for their invaluable guidance. I would like to thank them for their constant encouragement, constructive suggestions and comments which were vital in shaping up this work.

I am highly obliged to Dr R. N. Biswas (Prof E.E) for his help in the design of the electrical controls.

My thanks are due to all the persons of the Manufacturing Science Lab, particularly Mr Jha and Mr Bajaj. I am grateful to my friends in the Robotics Lab and others, to mention a few, Mandal, Seshadari, Avadhesh and Gawahale.

ABSTRACT

In the present work, a three-link arm is developed using Shape Memory Alloy wires for its actuation. This arm can move from one position to another and back,repeatedly. This motion has reasonable accuracy and repeatability as has been experimentally verified. It has low load carrying capacity. This arm is controlled by a Personal Computer using a digital output card with the necessary electrical interface.

TABLE OF CONTENTS

LIST OF FIGURES AND TABLES

Table No.

List of Symbols

M_s	Martensitic start
M_f	Martensitic final
A_s	Austenitic start
A_f	Austenitic final
T_d	deformation temperature
ε	strain
σ	stress
γ	deflection
θ	single variant

CHAPTER I

INTRODUCTION

1.1 INTRODUCTION

The state - of - art in the actuation of robots is by utilizing hydraulic motors,DC servomotors and to a lesser extend the stepper motors. But, the above methods have their own difficulties and limitations. Hydraulic motors are costly even though they give good accuracy in control.DC servomotors increase the weight at the joints of the robot or else transmission system is required if they are not fitted at the joints.The transmission system causes mechanical problems of backlash and increased manufacturing complexities. The stepper motors cannot give large torques. Thus, an unconventional approach was sought for which uses a peculiar alloy wire having shape memory effect(SME). The wire on heating contracts considerably giving a large force. The amount of contraction is temperature dependent. The SME wire is light , accurate in control and gives a large force.Thus, a number of uses in actuation for robots can be found.

The limbs of the humans are moved by the muscles which contract by the required amount on receiving an electrical signal from the brain. The human arms can carry a lot of load. The present work has derived the idea of this human arm which has had millions of years of test.The robot arm to be produced would utilize shape memory alloy (SMA) wires for its actuation.The links of this arm would be flexible so that they bend on actuation by SMA wires and a large work volume can be achieved.

1.2.1 BASIC STRUCTURE OF ROBOTS

Robots, as other modern manufacturing system, are advanced automation system that utilize computer as an integral part of their control .The robot is an automatic(without human intervention), reprogrammable(can be programmed again and again), multifunctional(able to perform more than one special duty) manipulator capable of moving along different directions , equipped at its end with a work device called an end effector and capable of performing work ordinarily done by human beings.

Modern robotics system consist of three major parts

(1) The manipulator which is the mechanical moving structure

(2) The drives to actuate the manipulator

(3) The computer as a controller and storer of task programs

1.2.1.1 THE MANIPULATOR

In general, the structure of a robot manipulator is composed of a main frame, a wrist and an end effector at the end of the robot. The main frame is frequently denoted as the arm which consists of a series of mechanical rigid links and joints. The joints are mostly revolute or prismatic. The arm gives the required position with controlled joint movement. A typical wrist which has three joints give the roll, pitch and yaw. The number of joints in the manipulator give the number of degrees of freedom of the robot.

1.2.1.2 DRIVES FOR ROBOTS

Drives for robot systems are mainly :

(i) Hydraulic -These are used for driving high power robots since they can deliver large power while being relatively small in size. They also offer accurate control. But these systems are more expensive as they need a control distribution unit and good amount of maintenance. These drives are not suitable for high speed cycling.

(ii) Direct current servomotors - This electrical drive offer accurate, reliable and fast control and are relatively inexpensive. Torque to weight ratio of these motors is a major disadvantage and if these are located away from the articulation location then these require gear trains for power transmission which bring in mechanical backlash.DC motors allow precise control of either the speed ,by manipulation of the voltage or the torque , by manipulation of the current applied to the motor.

(iii)Stepper motors - These are used only for small robots because the allowable speed of a stepping motor is a function of its load torque.

1.2.1.3 POWER SOURCES FOR END EFFECTOR

End effectors can also be similarly powered by the three methods discussed above in actuation of the joints of the arm. Pneumatic power can also be utilized for end effectors.These are easiest to use but are least sophisticated as servo controlled pneumatic systems are difficult to regulate. These cannot be used for high load operation.

1.2.2 CONTROL LOOPS FOR ROBOTS

Control systems can operate either in an open loop or a closed loop .In an open loop control system, the output has no effect on the input. A better system is the closed loop in which the output is sensed and fed back to be compared with the input variable .Based on this comparison, any necessary corrective action automatically takes place.

Most small to medium robots utilize DC servomotors as actuators. Two alternative approaches exist for control of this actuator. The first is to control torque of the robot arm by motor current . The second approach is to control the speed of the motor by manipulating the motor voltage.

1.2.3 ADVANTAGES AND APPLICATIONS

The robots are ideally suited for jobs which are regarded as unpleasant or unhealthy for people. Robots are ideal for any repetitive job which is regarded as too boring or too tedious for human operators.Robots are however useless for any intelligent work in which the creative abilities of a human being are needed.

The advantages of robots are

(a) Flexibility- The ease in which the robot with a little changein programming and step is able to produce a totally different finished product.

(b) High productivity -The faster rate of production by the use of robots has increased the productivity in industries.

(c) Better quality of products - With the precise control better accuracy of the output is achieved and this is provided by the use of robots.

(d) Improved quality of human life by performing undesirable jobs - All hazardous and undesirable work for the human being are done by the robots.

The applications of robots are

(a) Loading and unloading of machines

(b) Spot welding

(c) Spray painting

(d) Assembly

(e) Inspection

(f) Arc welding

(g) Die casting and forging

(h) Drilling and deburring of metal parts

1.3 A REVIEW ON SHAPE MEMORY ALLOYS (SMA)

1.3.1 INTRODUCTION

A shape memory alloy is one which has a highly twinned structure (martensite) at a lower temperature and at a higher temperature it has a B.C.C structure (austenite). A deformation made in the martensite can be fully or partially recovered on heating the alloy from its martensitic state to its austenitic state.Thus, the original shape of the alloy is reached at the higher temperature with any deformation caused at the lower temperature. For more details see chapter 2.

1.3.2 APPLICATIONS OF SHAPE MEMORY ALLOYS (SMA)

By controlling the alloying elements in SMA metals to occur at precise temperatures, enabling use of SMA in devices including thermostats, switches, actuators and couplings.

1.3.2.1 GRIPPER HAND AND ROBOT

The figure.1.1 shows a three fingered gripper made by Hitachi of Japan. It is quite versatile gripper made from light weight SMA and exhibiting human like flexibility.The figure 1.2 shows the robot arm actuated by Biometal wire at the joints(courtesy Toki Corporation,Japan).

1.3.2.2 ACTUATORS

SMA materials are finding use as actuators in place of motors or solenoids. These can be used for opening and closing of vents.

1.3.2.3 SENSORS

The thermal response capabilities of SMA open up many potential sensing applications. An example is a NiTinol actuated automatic water sprinkler for putting off room fire.

1.3.2.4 BIOMEDICAL

NiTinol can be used for such medical uses as compression plates for internal fracture.The transition temperature could be adjusted to body temperature .It is also corrosion resistant and compatible with tissues.

1.3.2.5 HYDRAULIC COUPLING

Hydraulic tube couplings are fabricated from the NiTinol alloy that has a martensite-formation temperature, Ms, in the

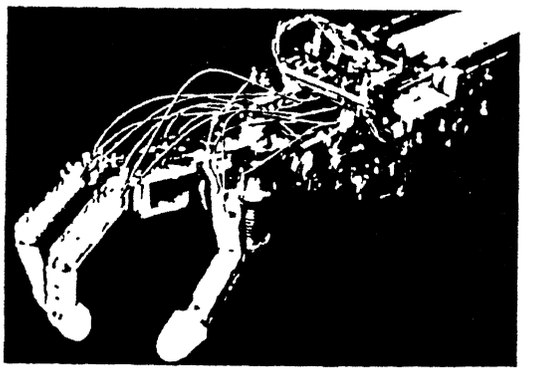

Figure 1.1 Three-fingered robotic gripper
(Courtesy of Hitachi, Japan)

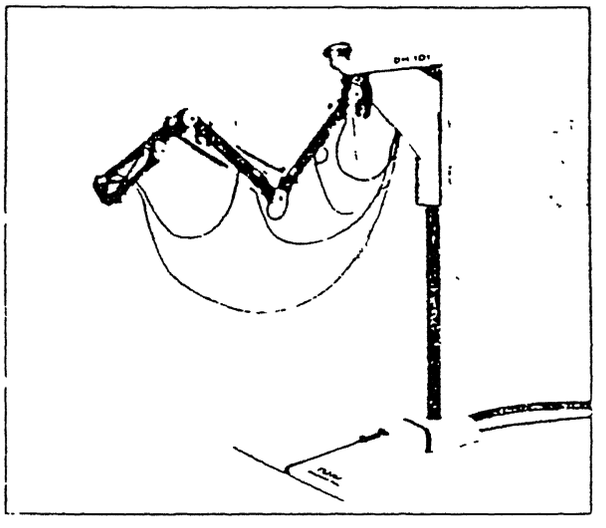

Figure 1.2 Biometal Actuated Robot
(Courtesy of Toki Corp., Japan)

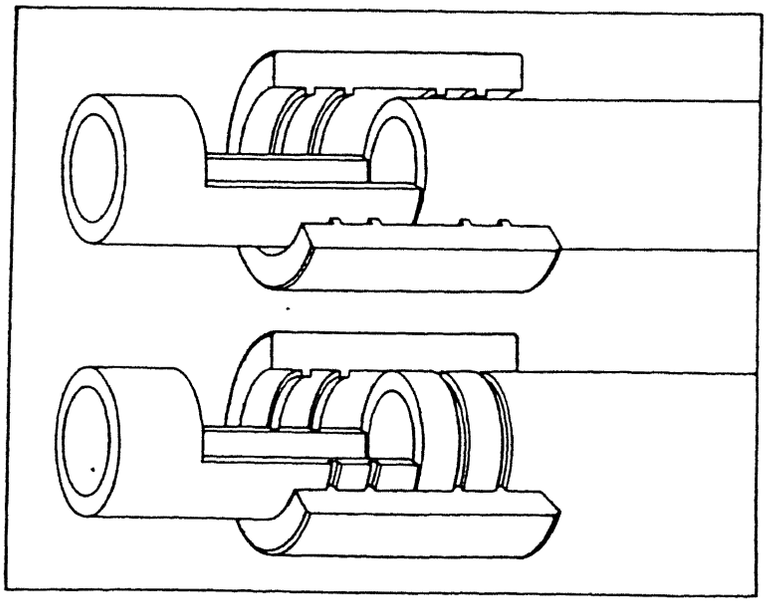

Figure 1.3 Hydraulic- tube coupling

cryogenic region below -120^{o}C [8]. The sleeve like coupling as shown in figure 1.3 is machined at normal temperature to have an inner diameter 4% less than the outer diameter of the tubes to be joined. The sleeve is then cooled below the Ms temperature and is mechanically expanded to have an inner diameter 4% greater than the tubes outer diameter. Still held at a temperature below Ms, the sleeve is placed around the ends of the tubes. When the coupling is warmed, it shrinks to form a tight seal. Ribs machined into the sleeve enhance seal by "biting" into tubes.

1.4 OBJECTIVE OF THE PRESENT WORK

The present robots have rigid links which are fixed at joints. The actuation is done at the joints which cause rotation or translation of the link. This system is quite bulky.An arm would be fabricated which would have flexible links instead of conventional rigid links. The actuation to this flexible link would be done by SMA wire which would bend the link. There would be no rotation at the joint but the link itself rotates.

A robot arm is to be designed, fabricated and then experimented upon to see its viability as a robot arm with SMA wire or biometal wire as an actuator. This arm will have a personal computer as its controller.An interfacing circuit would also be required. Thus, it is expected that the arm which would be consisting of three links would be able to reach a desired position with inputs through a PC. It would also move from one point to another point and back repeatedly.

1.5 ORGANIZATION OF THE WORK

The present work has been written into six chapters with chapter 1 giving a brief introduction on robotics and on the objective of the present work. Chapter 2 deals solely with the working of SMA metals and their properties. In chapter 3 the mechanical design for the different parts of the arm has been analyzed. In chapter 4 the electrical interface for the arm with the PC has been explained. The experiments done with SMA and biometal wire as actuator are explained and discussed in chapter5. Chapter 6 concludes the present work.

CHAPTER II

BASICS OF THE SHAPE MEMORY ALLOY

2.1 INTRODUCTION TO SHAPE MEMORY ALLOYS (SMA)

The term SHAPE MEMORY has been used to describe a wide variety of effects but in all of them the shape at a high temperature is recovered after deforming the specimen at a lower temperature to a different shape and reheating to the original temperature. The two major groups of alloys which exhibit this effect are binary alloys of transition metals,one component to the left and the other to the right of chromium and Beta phase alloys of the precious metals. Most of them have CsCl structure at the high temperature and all transform martensitically to a low temperature phase with a lower symmetry. The example of the first group is NiTi and of the second group is AuCd.

2.2 DEFINITIONS

2.2.1 INTRODUCTION

This sub-section highlights the different properties of SMA metals which are shape memory effect, superelasticity, ferroelasticity. It also mentions the temperature region in which they occur. Trainability has been included as this is the method which is used to change the property of SMA metal from shape memory effect (one way) to the reversible effect (two way).

2.2.2 SHAPE MEMORY EFFECT (SME)

A material apparently plastically deformed at a suitable temperature recovers, fully or partially, its original shape on subsequent heating to a moderately higher temperature [1]. Strains

of up to 8 - 10 % can be thus fully recovered. The magnitude of the recoverable strain varies with the material and for a given grain size, texture and the conditions under which strain is affected. Subsequent cooling to the temperature at which deformation took place does not restore the specimen to its deformed configuration. A sound scientific terminology for SME would be thermoelastic martensitic reversion or martensitic thermoelasticity.

2.2.3 SUPERELASTICITY (PSUEDOELASTICITY)

A material deformed well past its apparent yield point fully recovers its initial shape on removing the load. Significant stress strain hysteresis, indicative of energy absorption in the lattice is observed [1]. This behavior is due to the stress assisted martensite formation during loading (stressed condition) but martensite is thermally unstable so the temperature range observed is Af < T < Md. On unloading there is reversion to the initial structure and orientation.

2.2.4 FERROELASTICITY

A stress strain behavior like superelasticity but occurring in material stressed while in fully martensitic condition [1]. There is stress assisted growth of the martensite lamellae of one orientation at the expense of similar lamellae of the other orientation (widely interpreted as reversible twin boundary motion).

This property is produced after training the SMA wire and TiNi Alloy Company, U.S.A markets this trained wire in a trade name of Biometal.

2.2.5 TRAINABILITY

Training is accomplished by limiting the number of variants of martensite formed when an alloy is repeatedly heated and cooled below the critical temperature [8]. The number of variants can be limited by stressing the specimen while it is cooling from the elevated temperature of the Beta phase down to the critical temperature. The stress favors the initial formation of particular variants of martensite in the same way that stress at constant temperature favors the growth of one variant at the expense of another. Hence a structure can be trained by repeating many times the sequence of Betatizing i.e.heating the alloy to Beta phase, quenching, deforming and Betatizing again. Thus, 'Two Way ' memory is achieved.

2.3 THERMOMECHANICAL CHARACTERISTICS OF ALLOYS EXHIBITING MARTENSITIC THERMOELASTICITY

2.3.1 PARAMETERS IN SME

ε_1 = Initial martensitic strain for (A $\rightarrow$ Md) or (Mt$\rightarrow$ Md)

where Md = stress induced martensite

Mt = athermal martensite

$\varepsilon_1 = \varepsilon - \varepsilon_e$

where ε_e = elastic strain component

ε = initial strain

ε_r = reversion strain

$\varepsilon_{r(SE)}$ = immediate (superelastic effect) reversion strain

$\varepsilon_{r(SME)}$ = heating activated (shape memory effect) reversion strain

$\varepsilon_f = \varepsilon_1 - \varepsilon_r$ if ($\varepsilon_1 < \varepsilon_l$)

ε_f = residual strain after heating above austenite (A)

εl = strain limit

% strain recovery = $(\varepsilon r / \varepsilon l) * 100$

σr = reversion stress (developed on heating above Af when all or part of εr is constrained against recovery)

εr (FREE) = unconstrained reversion strain

εr(CON) =constrained reversion strain

$\varepsilon r(CON) = \varepsilon l - \varepsilon r(FREE)$ if $(\varepsilon l < \varepsilon l)$

$\varepsilon r(CON) = \varepsilon l - \varepsilon r(FREE) - \varepsilon f$ if $(\varepsilon l > \varepsilon l)$

$\sigma a \rightarrow m$ = flow stress for stress induced reaction A→ M

$\sigma m \rightarrow a$ = flow stress for reversion reaction M→ A on reversal of stress sense starting in stress induced martensite state

$\sigma m \rightarrow mp$ = flow stress for true plastic deformation of stress induced martensite

Md =temperature where $\sigma A \rightarrow M$ (transformation yield point) equals $\sigma A \rightarrow Ap$ (true plastic yield point).

Referring to figure 2.1 ,$\sigma A \rightarrow M$ decreases with decreasing temperature above Ms due to increasing instability of parent A phase and becomes approximately zero at Ms [3]. Similarly, $\sigma M \rightarrow A$ decreases with decreasing temperature above As and becomes approximately zero at As, with the explanation that when Td (deformation temperature) is closer to As stress induced thermoelastic martensite is more stable, so that stress must be reduced to a lower level before reversion to parent A phase is possible. At Td< As, there will be no immediate reversion at all

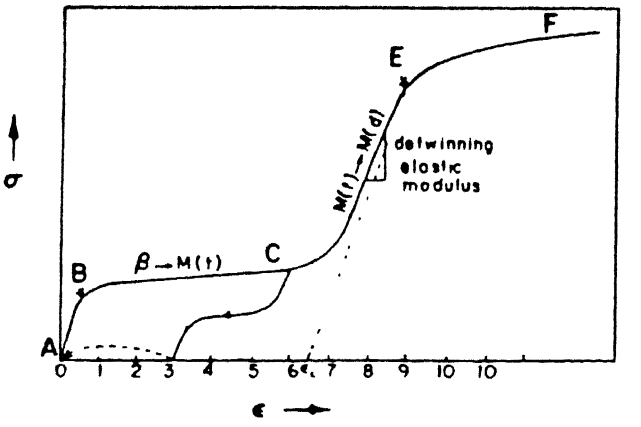

Figure 2.1 Typical stress-strain curve for SME alloy at As<Td<Af<Md. Point B: $\sigma_{A\to M}$. Point E: true plastic deformation begins.

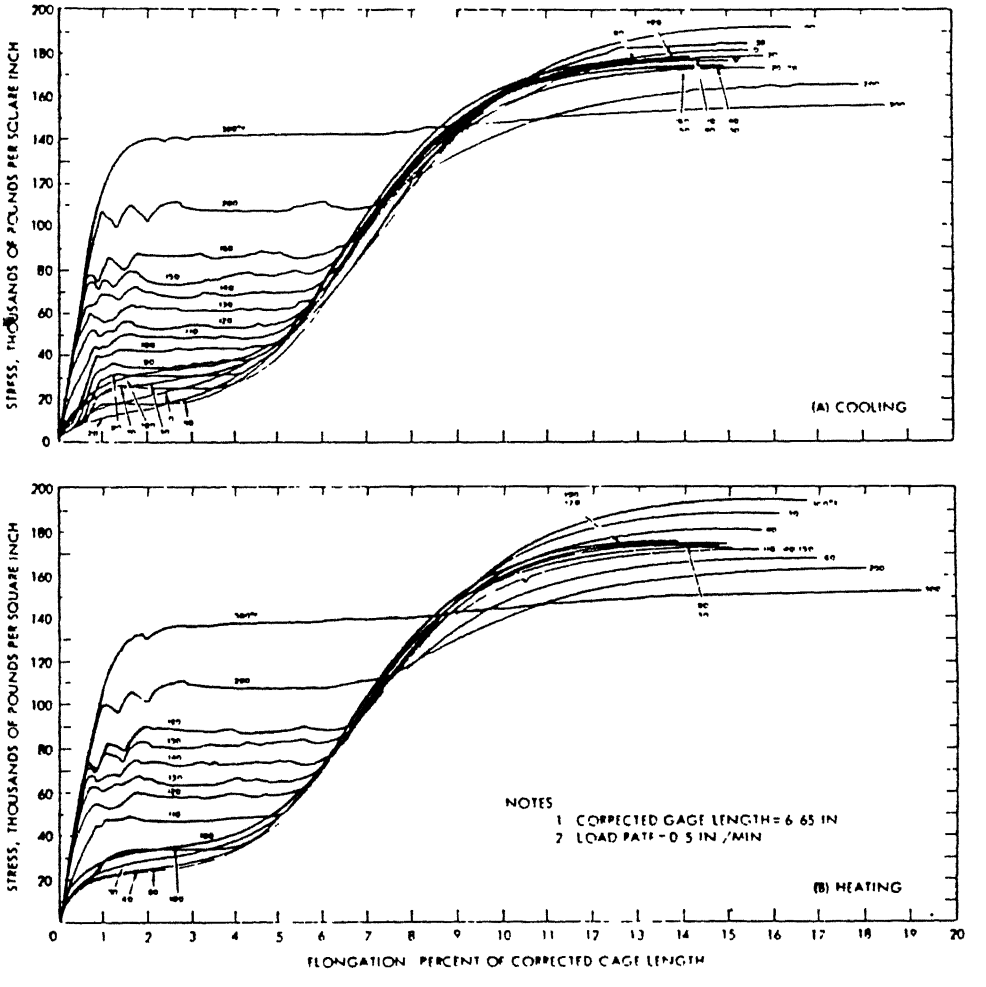

Figure 2.2 Stress-elongation curves as a function of temperature for NiTi, during cooling and heating cycles (from Ref. 3).

and thermal activation of M →A reaction by heating will be required i.e. only SME behavior will occur. Temperature dependency of the yield point for the true plastic deformation reaction (M→ Mp, A→Ap) show a classical increase with decreasing temperature [3].

The most interesting parameters relative to application of thermoelastic martensite effect are reversion strain and reversion stress.

2.3.1 REVERSION STRAIN - (Shape Recovery)

One of the primary parameters useful for application for thermoelastic martensitic effects is εr, the ability to return towards $\varepsilon=0$ [3]. Assuming $\varepsilon i<\varepsilon 1$ and no external constraint then $\varepsilon 1=\varepsilon r$. Referring to schematic hysteresis loop,the two extreme deformation ranges can be defined as

Af < Td < Md, $\varepsilon r= \varepsilon r(SE)$

Td < As < Md, $\varepsilon r= \varepsilon r(SME)$

In a more general case,

As<Td<Af<Md

$\varepsilon = \varepsilon r(SE) + \varepsilon r(SME)$

(1 - F)(M(t)) → A superelastic effect

(F)(M(t)) → A shape memory effect where

F = (Af - Td)/(Af - As)

Thus, if Td = Af, F=0 complete superelasticity

if Td = As, F=1 complete shape memory effect

Figure 2.2 shows the stress induced martensite formation versus elongation at different temperatures. It can be seen that stress and temperature govern the thermoelastic martensite.

2.3.2 STRAIN LIMIT

There is for each SMA metal a strain limit εl, a critical value of initial martensite strain (εi) beyond which many of the desirable parameters deteriorate(see figure 2.3), these include decrease in % strain recovery, maximum obtainable reversion strain and potential work output [3].

Experimentally εl is always greater for single crystal than for polycrstalline material of the same alloy. This is due to constraint of grain boundaries on stress induced martensite deformation process which require mobility of martensitic structural features and this value decreases with increasing εi until stabilization or perfect repeatability is produced.

2.3.3 CYCLING EFFECT ON REVERSION STRAIN (εr)

In SME cycling i.e., deformation to a given strain εi in each cycle, heating to just above Af in each cycle it shows a gradual decrease in % strain recovery with increasing cycles as shown in figure 2.4 [3]. This value also decreases with increasing εi until stablization is reached.

2.3.4 REVERSIBLE (TWO WAY) EFFECT

Reversible SME have been reported in which an alloy remembers both high and low temperature shapes (strain positions). There is no hysteresis during temperature cycle. This effect is reported from all alloys in which usual one way memory occurs [3].

The most pronounced two way effect are observed in cases where an alloy is deformed severely and non uniformly such that some fibers exceed strain limit for complete recovery,εl, and

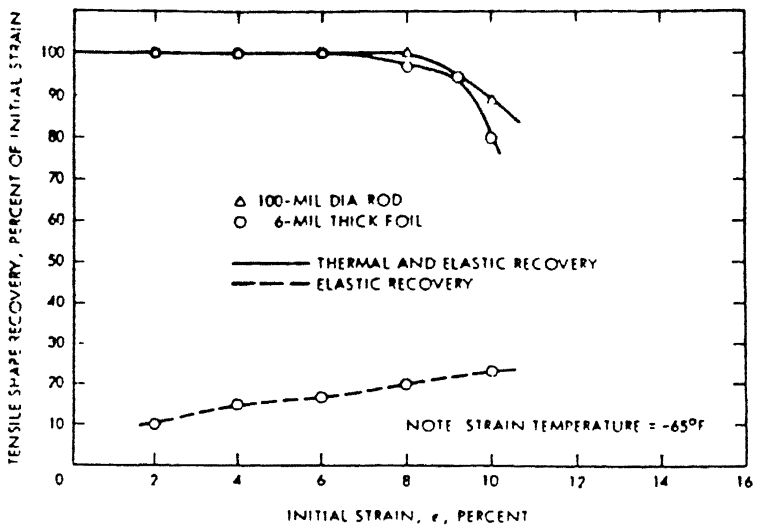

Figure 2.3 Percentage strain recovery [%R = ($\varepsilon_r/\varepsilon_i$) x 100] versus ε_i for NiTi, showing a decrease in %R beyond ε_L (from Ref. 3).

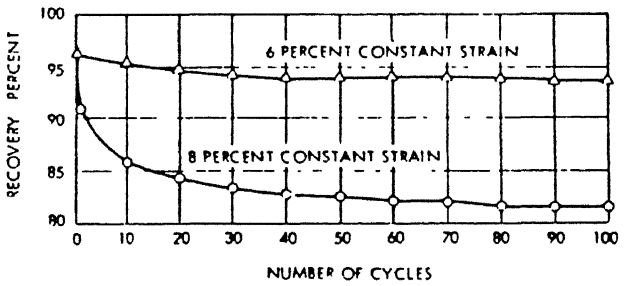

Figure 2.4 Percentage strain recovery versus number of SME cycles (deform below Mf, heat above Af) for NiTi, showing the attainment of perfect repeatability with cycling (from Ref. 31).

others do not. Those regions where εl has been exceeded will develop residual stresses on heating above Af as some fibers will be constrained from full reversion. The residual reversion stress (σr) is proportional to retained unreverted strain $\varepsilon r(CON)$. If the alloy is cooled below Md, this residual stress pattern will stress induce martensite in a pattern of appropriate orientation to accommodate the stress. Fibers in residual compression will shorten and fibers in residual tension will elongate, giving rise to a net shape change that will tend towards the initial deformed low temperature shape. In general complete recovery of both high and low temperature shapes is difficult.

2.3.5 REVERSION STRESS σr

If the initial strain εi is constrained to prevent reversion, significant internal stress will be developed on heating through the As-Af range, er increases in sigmoidal fashion over this range [3]. The maximum reversion stress $\sigma r(max)$ is a function of εi, increasing with εi till εl and then decreasing for fully constrained case. And, $\sigma r(max)$ is a linear function of final constrained strain value, at a given deformation temperature if $\varepsilon i < \varepsilon l$. See figure 2.5 for furthur details.

The reversion stress at any temperature between As and Af during build up towards $\sigma r(max)$ is a function of residual transformation strain in a sample at a given temperature. The reversion stress can be approximated by the flow stress at that temperature as an upper bound. For a given εi, $\sigma r(\varepsilon i, T)$ during cooling is the reversion stress exhibited for prestrain at a

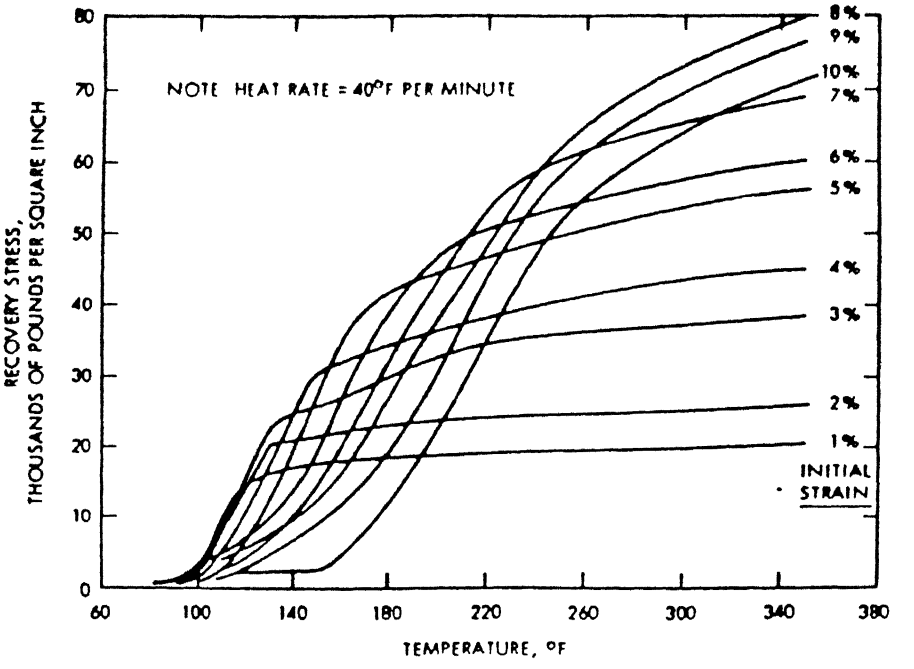

Figure 2.5 Reversion stress, σ_r, versus temperature during heating for various ε_i for NiTi, showing increasing $\sigma_{r(max)}$ (below ε_L) and upward-displaced reversion temperature range with increasing ε_i (from Ref. 3.)

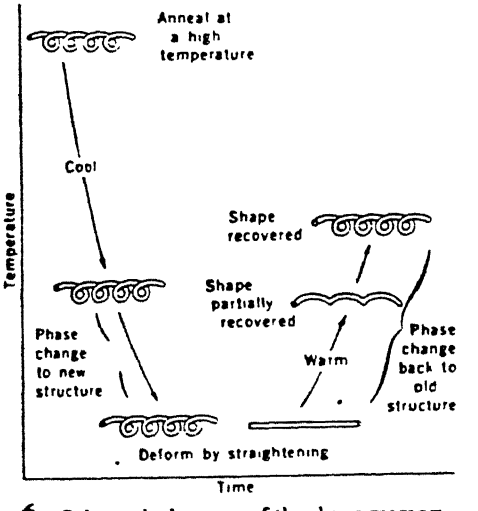

Figure 2.6 Schematic diagram of the shape memory effect. Annealing at a high temperature "fixes" the permanent shape. After being deformed into any other shape at a low temperature, the alloy returns to its permanent shape upon being warmed up.

given temperature and is a measure of stability of martensitic phase at that temperature, so is directly related to the stress required to induce the same amount of transformation strain at that temperature.

2.3.6 STABILITY OF REVERSION STRAIN

The ability to maintain a significant and constant value of reversion strain may be required in some application [3]. Two situations in which are er might deteriorate are :

(i) During prolonged maintenance of temperature above Af

(ii) During subsequent reduction of temperature to below Md or Ms.

In the first case if stress generated by constrained reversion reaction $\sigma r(M \rightarrow A)$ exceeds $\sigma A \rightarrow$ Ap duringreversion heating, the high temperature phase will yield limiting further stress elevation and true plastic strain is produced. Also, moderate heating above Af while in constrained condition [$\varepsilon r(CON), \sigma r$] could seriously degrade subsequent shape recovery capabilities.

In the second case where an external load is maintained true plastic deformation may occur as the internal σr decreases while cooling. This is due to drastic decrease in the yield stress as the alloy approaches Ms [3].

2.4 MECHANICAL PROPERTIES OF SME ALLOYS

In case of SMA metals most of the recoverable strain is associated with the reversible martensitic formation and is due to macroscopic shear strain caused by the transformation [2].

The stress necessary to initiate martensite decreases linearly with temperature becoming zero at Ms. The variation of

σ_A with temperature can be calculated from the Clausius - Clapyron type equation applicable to stress induced martensite (SIM).

ΔH- heat of transformation

ΔE - strain corresponding to complete transformation to

To - temperature at which matrix and martensite phases are in equilibrium at zero stress

Vm - molar volume

This formula is based on a balance between volume free energy and mechanical work in the transformation. It assumes zero hysteresis in the stress-strain curve.

$\Delta\sigma_A / \Delta T = \Delta H/(\Delta E*To*Vm)$

2.4.1 EFFECT OF STRAIN RATE

The shape of superelastic stress-strain curve depends upon the rate of straining the specimen [2]. This is due to significant temperature changes which take place in the specimen at high strain rates which is due to the heat of transformation(ΔH). There is temperature rise during parent-martensite transformation and temperature decreases during reverse transformation . The maximum temperature change is given by

Cp- specific heat of martensite formation (forward\reverse)

$\Delta T = \Delta H / Cp$

2.4.2 EFFECT OF GRAIN SIZE

The polycrstalline specimen have inferior superelastic properties compared with single crystals since in single crystal

only one martensite variant need form whilst in polycrystals several variants (generally 5) must form in different regions of any given grain to allow for effects of constraint from adjacent grains [2]. The stress concentrations due to presence of the grain boundaries produce non- reversible deformation martensite and prevent full development of superelastic effect.

2.3 WORKING PRINCIPLE OF SHAPE MEMORY ALLOY

All SMA metals exist in two phases, one at a high temperature and another at a low temperature. The highly symmetric CsCl structure, with one atom of the binary alloy at each corner of the simple cubic unit cell and the second atom at the center i.e., Body Centered Cubic structure, is by far the most common structure of the high temperature phase [4]. The low temperature phase exhibits a lower symmetry i.e., highly twinned structure.

A SMA metal can be formed into the desired configuration, for example, a spiral as shown in the figure 2.6, and may also be annealed the specimen at some elevated temperature to fix the shape. The crystal structure changes as the alloy cools. At the low temperature, the specimen is reshaped, for example, by straightening the spiral [10]. Upon heating to a temperature above the high temperature phase but well below the annealing temperature, the alloy returns to its first shape i.e., spiral. Considerable force can be generated during the shape change.

The temperature range over which the transition from high to low temperature phase of the SMA occurs is determined by the relative proportion of Nickel and Titanium in the alloy. A wrought stoichiometric alloy of commercial purity with 50% Ni and

50% Ti transforms in the temperature range 385 to 400K. Increasing the Ni content lowers the transition temperature range in the neighborhood of 190K. Substituting small amount of Cobalt or Iron for Ni can lower the transition temperature range to liquid nitrogen temperature [10].

Figure. 2.8 shows the relationship of the length of the Nitinol wire to the stress or force applied in this relaxed state. Starting at point O of no force and no elongation, the wire elongates with the increase of force and then at some stressvalue starts elongating with this stress remaining applied [9].After this as further increase in considerable amount of force takes place, the wire elongates by a very short length.

In the hot state(temperature 100^{o}C) the Nitinol wire reacts very much like a strong spring, elongating only as sizable forces are used to deform it. The wire changes length linearly with the applied force [9]. On unloading the wire returns by a slightly different path due to hysteresis as shown in figure 2.8.

2.6 WORKING PRINCIPLE OF THE BIOMETAL WIRE

Biometal is the trade name for a very sophisticated Titanium-Nickel alloy. The name Bio correlates the lifelike characteristics of the muscle when electrically heated. There are two extreme states, the cold (relaxed) state and the hot (contracted) state of the Biometal [9]. The hot phase begins to occur at about 100^{o}C and is completed around 130^{o}C, varying slightly based on stress.

Figure. 2.7 shows the relationship of the length of the wire to the stress or force applied in this relaxed state.

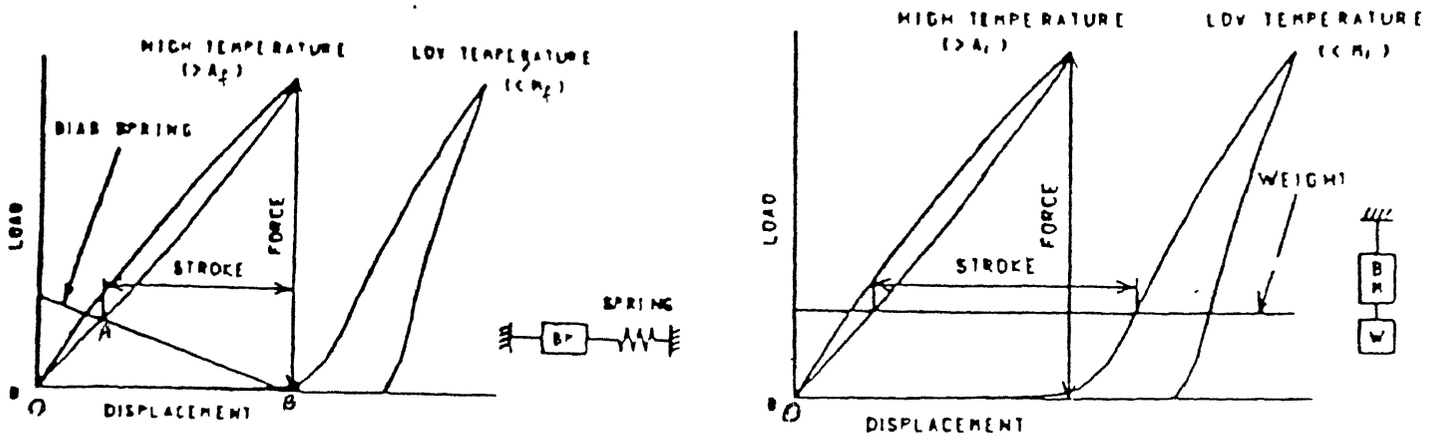

Figure 2.7 Load-Displacement-Bias Comparisons for Biometal wire

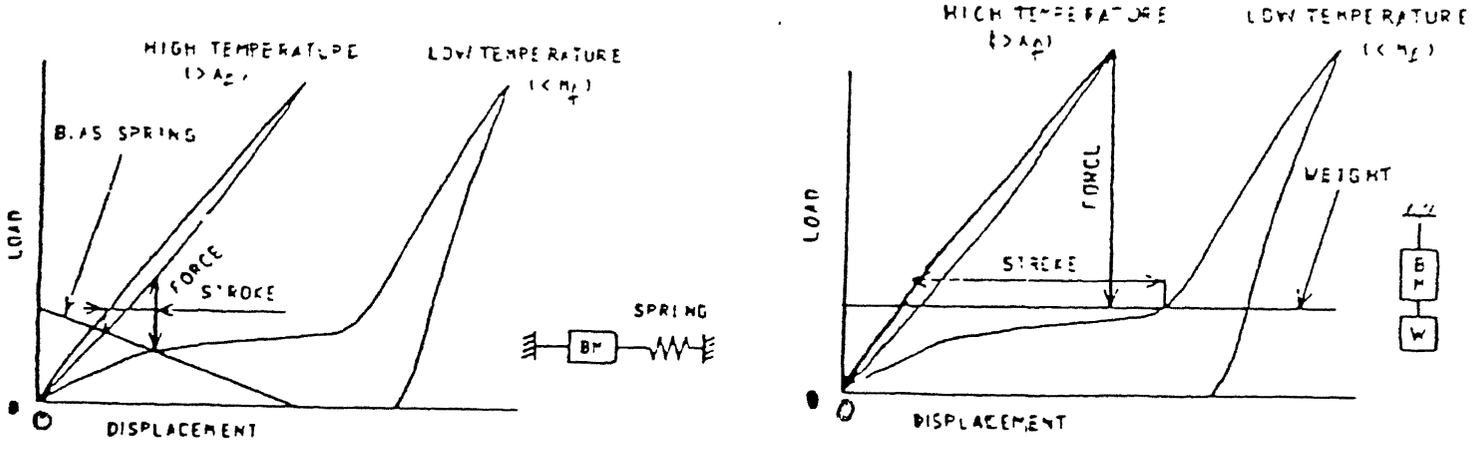

Figure 2.8 Load-Displacement-Bias Comparisons for Nitinol Wire

Starting at point O of no force and no elongation, a small force is applied to elongate the wire and the wire gives way. After this even if the forces increase many times, the wire elongates by a very short length.

In the hot state the wire reacts very much like a strong spring, elongating only as sizable forces are used to deform it. The wire changes length linearly with the applied force. On unloading the wire returns by a slightly different path due to hysteresis [9].

Since some force must be applied to stretch even a relaxed wire fully, a bias force must be applied. This bias force can be in the form of a spring or weight. When a spring is used as a bias force to stretch Biometal in the relaxed state it must be working in reverse. This is shown in Fig.2.7. Movement in this case occurs between points A and B along the curve of elongation vs force of the spring.

Electrical heating of the Biometal can be done in a number of ways, with A.C, D.C, or pulse width modulation, which works well for fine control.

2.7 DIFFERENT MATERIALS EXHIBITING SME

SME has been discovered in a number of alloy systems. The most widely known and developed alloys are the NiTi based NiTinols. Other systems in which the SME is ~~know~~ known to occur include InTl, CuZn, CuAl, NiAl, Fe_3Pt, AgZn, AgCd and other alloys based on some ~~some~~ of these systems. These are CuAlNi, CuZnSi, CuZnSn and CuZnAl. The primary requirement for the SME occurrenceis the presence of thermoelastic martesitic transformation [3].

CHAPTER III

MECHANICAL DESIGN

3.1 INTRODUCTION

A different approach is employed to design the links of the robot arm from the conventional strategy of having rigid links. Here the link to be designed is required to be flexible so that it can bend when actuated by the SMA wire. The bending of the link will give the required displacement to the free end of the link. This displacement is a function of the amount of contraction in the SMA wire.

This chapter deals with the method of selecting the fixing arrangement of the SMA wire to the link and the method of selecting the configuration of the arm. Then a force analysis is done to find the amount of tension in each link of the robot arm. Later the way in which the steel link and the composite link is made is discussed. At the end the method of designing and fabrication of a gripper is presented.

3.2 DISPLACEMENT ANALYSIS OF A SINGLE LINK

The basic requirement of the link to be designed is to have a large movement at the tip which would give the robot arm a large work volume. Two arrangements of fixing the wire are possible, these are analyzed and discussed below.

In this first arrangement as shown in the figure 3.1 the SMA wire is fixed to the end of the link but there is no restriction that the wire will keep a constant distance with the link plane. It is assumed that the link attains a constant curvature when SMA

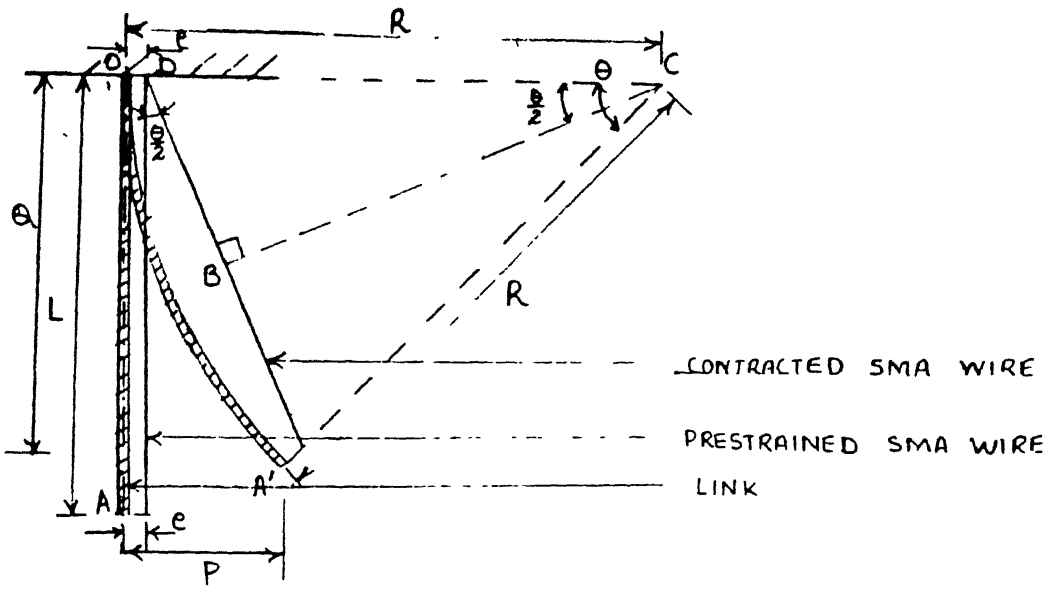

Figure3.1SMA Wire fixed to link ends

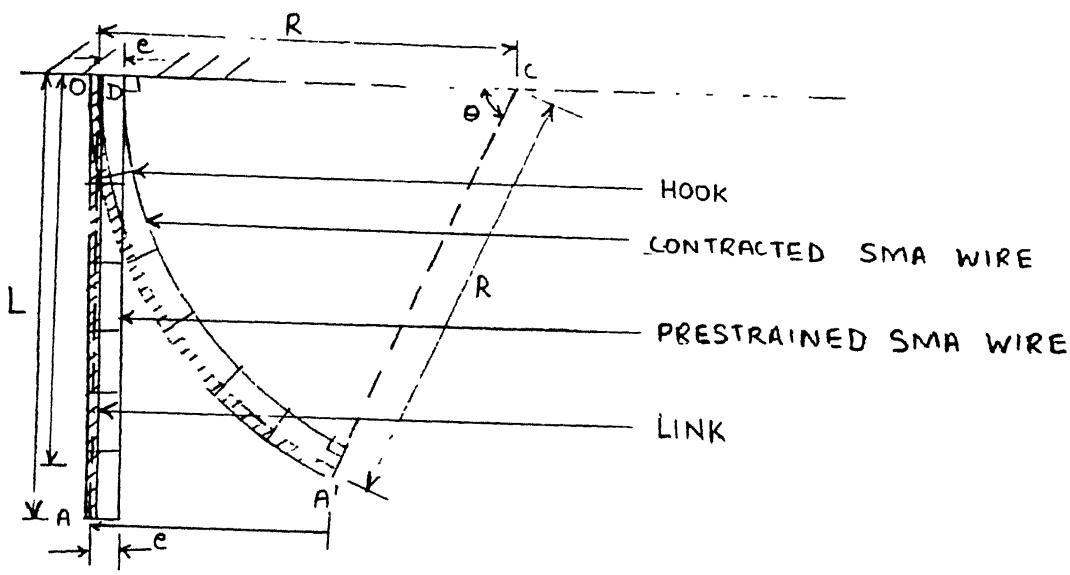

Figure 3.2 SMA Wire fixed to link ends with hooks

wire contracts i.e from its initial position at OA to the final position at OA' as shown in the figure 3.1. Now the analysis is made to find the rotation (θ) produced for a required strain in the link.

Let

L = length of the link

θ = sector angle as link has circular curvature

ε = strain in the SMA wire

e = distance between SMA wire and link plane

R = radius of curvature

Now

$$L = R\theta \qquad (1)$$

From triangle BCD by geometry

$$\frac{L}{2}(1-\varepsilon) = (R-e)\sin\frac{\theta}{2} \qquad (2)$$

Using equation 1 in equation 2

$$\frac{L}{2}(1-\varepsilon) = (\frac{L}{\theta} - e)(\frac{\theta}{2} - \frac{(\frac{\theta}{2})^3}{3!})$$

$$L(1-\varepsilon) = (L - e\theta)(1 - \frac{\theta^2}{24})$$

$$L(1-\varepsilon) = L - e\theta - \frac{L\theta^2}{24} + \frac{e\theta^3}{24} \qquad (3)$$

Neglecting $\frac{e\theta^3}{24}$ as it is negligible

$$\frac{L\theta^2}{24} + e\theta - \varepsilon L = 0 \qquad (4)$$ thus, $$\theta = \frac{-e \mp (e^2 + \frac{L\varepsilon}{6})^{\frac{1}{2}}}{\frac{L}{12}}$$

The solution with $\theta<0$ is not possible so it is neglected

Thus, $$\theta = \frac{-e + (e^2 + \frac{L\varepsilon}{6})^{\frac{1}{2}}}{\frac{L}{12}} \qquad (5)$$

The above formula gives the sector angle for a given strain in SMA wire.

In the second method where the SMA wire is passing through hooks fixed to the link. In this method the wire will maintain a constant distance while in contracted state also. This system is shown in figure 3.2. The hooks are placed so that they do not allow the SMA wire on contraction to have a straight line configuration on contraction.

The initial position of the link is OA and final position is OA'. Now again an analysis is made to find the rotation (θ) produced for a required strain in the link.

In this case bending moment would increase from point A' to point O but assumption of constant curvature is made to make this analysis simpler.

$$L = R\theta \qquad (6)$$

$$L(1-\varepsilon) = (R- e)\theta \qquad (7)$$

subtracting equation 6 from equation 7

$$e\theta = \varepsilon L$$

Thus,

$$\theta = \frac{\varepsilon L}{e} \qquad (8)$$

The rotation by this method is more than that by the earlier method for same link dimensions and distance of the wire from link plane. Thus, this method is selected for fixing the SMA wire on the link, and all subsequent analysis are presented for the second type of configuration.

3.3 FORCE ANALYSIS OF A SINGLE LINK

With the link design selected as in figure 3.2 the SMA wire is fixed and held at a distance to the link axis, the contraction of the SMA wire will bend the link. Assuming the link curvature is in the form of a circular arc, the displacement of the free link end can be found as under.

From sec. 3.2 eq.8,

$$\varepsilon = \frac{e\theta_r}{L} \qquad (4)$$

$$R = \frac{L}{\theta_r} = \frac{e}{\varepsilon}$$

The displacement of the free end of the link is given by

$$y = R(1 - \cos\theta_r)$$

$$y = \frac{e}{\varepsilon}(1 - \cos\theta_r) \qquad (5)$$

To find the tension in the SMA wire, the method followed is firstly the displacement of end point of link caused by a force acting normally to the link is analyzed. Then the displacement of the end point of link caused due to a moment is analyzed. Assuming that superposition of force and moment holds good, the displacement of end point of link depends on the n different forces from n hooks and the bending moment. The free body diagram of the link is shown in figure 3.4.

Now assuming a link bend by only one force which is always acting normally to it as shown in the figure 3.5, the equation for bending can be written as

$$EI \frac{d^2y}{dx^2} = -M_x = -F\cos\phi \langle x - a\rangle - F\sin\phi \tan\phi \langle x - a\rangle \qquad (6)$$

where

E = Modulus of elasticity of link material

I = Moment of inertia of the link

y = Displacement of the free end of the link

F = Magnitude of the force

ϕ = Angle made between the initial position of link and tangent at the point of application of the force.

$\langle\ \rangle$ is a unit function i.e. if the inside value of this function is negative then value of the function is zero otherwise it is same as the inside value.

$$EI \frac{d^2y}{dx^2} = - F\cos\phi\ (1 + \tan^2\phi)\ \langle x - a\rangle \qquad (7)$$

After integrating,

$$EI \frac{dy}{dx} = - \frac{F\cos\phi}{2}\ (1 + \tan^2\phi)\ \langle x - a\rangle^2 + C_1 \qquad (8)$$

where C_1 = Constant of integration

Now Putting the first boundary condition i.e. $x = L, (\frac{dy}{dx})_{x=L} = 0$

$$C_1 = \frac{F\cos\phi}{2}\ (1 + \tan^2\phi)(L - a)^2$$

Hence,

$$EI \frac{dy}{dx} = - \frac{F\cos\phi}{2EI}\ (1 + \tan^2\phi)[\langle x - a\rangle^2 - (L - a)^2] \qquad (9)$$

Rotation of the free link end is given by

$$\theta_F = \frac{dy}{dx} = \frac{F\cos\phi}{2EI}\ (1 + \tan^2\phi)[(L - a)^2] \qquad (10)$$

Integrating eq. 9

$$EIy = - \frac{F\cos\phi}{2}\ (1 + \tan^2\phi)[\frac{\langle x-a\rangle^3}{3} - (L-a)^2 x] + C_2 \qquad (11)$$

where C_2 = Constant of integration

Now putting the second boundary condition i.e. at $x = l$, $(y)_{x=L} = 0$

$$C_2 = \frac{F\cos\phi}{2}\ (1 + \tan^2\phi)[\frac{(L-a)^3}{3} - (L - a)^2 L]$$

$$C_2 = -\frac{F\cos\phi}{6}(1+\tan^2\phi)[(2L+a)(L-a)^2] \quad (12)$$

Hence,

$$EIy = -\frac{F\cos\phi}{2}(1+\tan^2\phi)[\frac{\langle x-a\rangle^3}{3} - (L-a)^2x + \frac{(2L+a)}{3}(L-a)^2]$$

$$EIy = -\frac{F\cos\phi}{6}(1+\tan^2\phi)[\langle x-a\rangle^3 - (L-a)^2(3x-2L-a)] \quad (13)$$

The tension in the wire causes a compressive force and moment. The moment due to this compressive force is neglected from the equation given below for bending moment.

$M_x = Te + T\cos\theta\, R(1-\cos\theta) - T\sin\theta(R\sin\theta - x)$

Thus as assuming that only a moment is causing bending of the link as shown in the figure3.6.

By the Pure bending equation

$$EI\frac{d^2y}{dx^2} = -M_x$$

$$EI\frac{d^2y}{dx^2} = -M$$

Integrating $EI\frac{dy}{dx} = -Mx + C_3$ (14)

where C_3 = Constant of integration

Now putting the first boundary condition i.e.at $x=L, (\frac{dy}{dx})_{x=L}=0$

$$C_3 = ML$$

Hence,

$$EI\frac{dy}{dx} = -M(x-L) \quad (15)$$

Rotation of the free link end

$$\theta_m = (\frac{dy}{dx})_{x=0} = \frac{ML}{EI} \quad (16)$$

Integrating eq.15

$$EIy = -M(\frac{x^2}{2} - Lx) + C_4$$

where C_4 = Constant of integration

Now putting the second boundary condition i.i.at $x=L, (y)_L=0$

$$C_2 = M\left(\frac{L^2}{2} - L^2\right) = -\frac{ML^2}{2} \qquad (17)$$

Hence,

$$EIy = -M\left(\frac{x^2}{2} - Lx + \frac{L^2}{2}\right)$$

$$EIy = -\frac{Te}{2}(x - L)^2 \qquad (18)$$

As shown in the figure 3.2 the SMA wire is fixed at the ~~at~~ both ends of the link at the distance e apart from the link plane passing through n equally spaced hooks. Thus, n different forces act normally to the link through these hooks. SMA wire is fixed at the ends at a distance from the link axis thus it would cause a bending moment and the contribution of the compressive force on bending moment is neglected as specified above.

Therefore, for the arrangement shown in figure 3.2 the bending equation can be written by superposition of forces and moments as obtain in equation 7 and 1.

$$EI\frac{d^2y}{dx^2} = EI\left(\frac{d^2y_1}{dx^2} + \frac{d^2y_2}{dx^2} + \ldots\ldots\ldots + \frac{d^2y_n}{dx^2} + \frac{d^2y_M}{dx^2}\right) \qquad (19)$$

y_n = displacement caused by the nth force coming from the nth hook.

$$EI\frac{d^2y}{dx^2} = \sum_{i=1}^{n} -F\cos\phi_1\,(1 + \tan^2\phi_1)\,\langle x - a_1\rangle - Te \qquad (20)$$

where T = Tension in SMA wire.

And

$$EIy = EI\,[y_1 + y_2 + \ldots\ldots y_n + y_m] \qquad (21)$$

$$EIy = \sum_{i=1}^{n} \frac{F_1\cos\phi_1}{6}(1 + \tan^2\phi_1)[\langle x - a_1\rangle^3 - (L-a_1)^2(3x - 2L - a_1)] - \frac{Te}{2}(x-L)^2 \qquad (22)$$

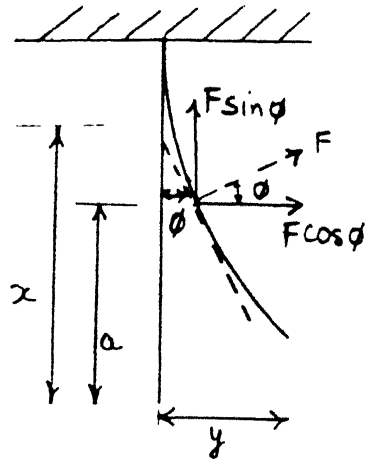

Figure 3.5 : Force causing bending of link

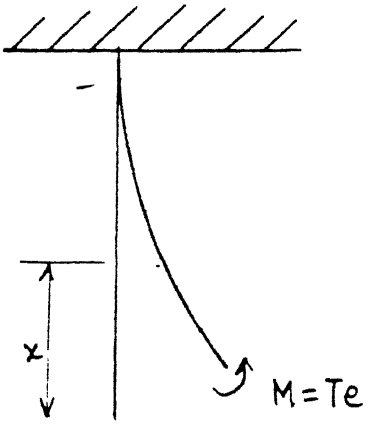

Figure 3.6 : Moment causing bending of link

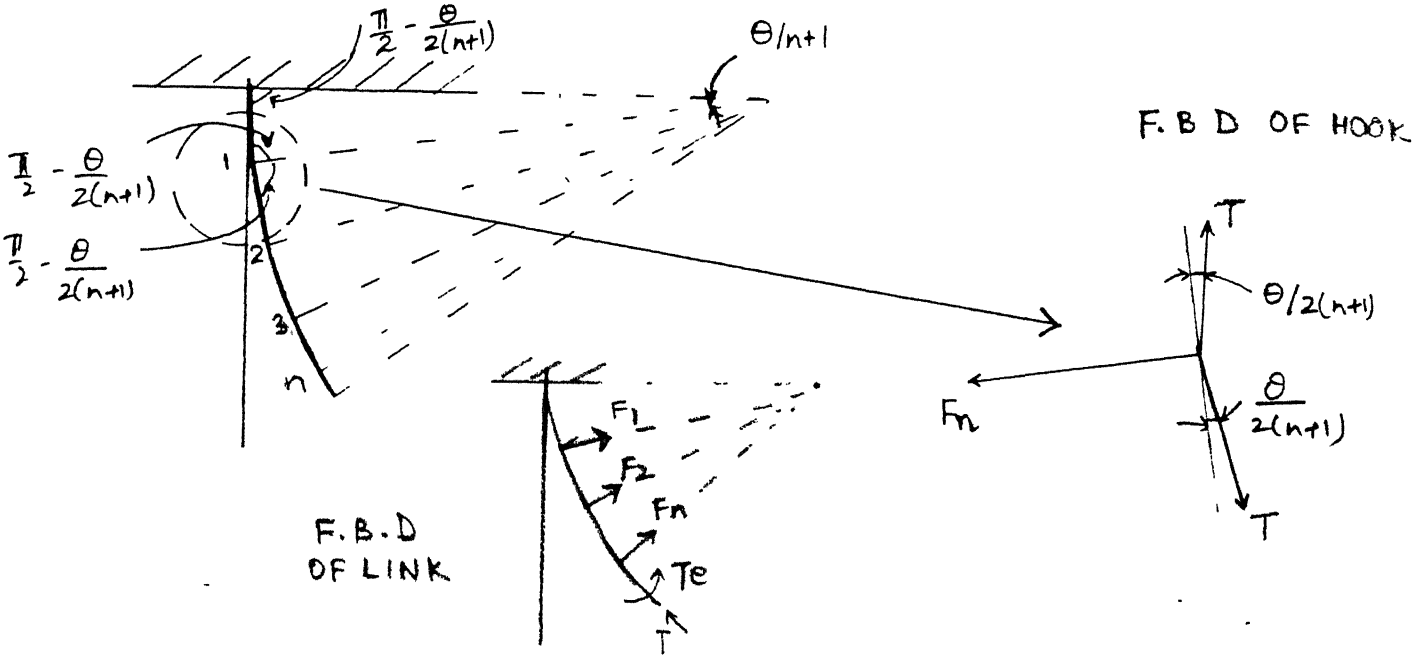

Figure 3.7 : Tension in wire versus force in hook.

Now finding the relation between the n forces and the tension in the SMA wire.

The free body diagram of the nth hook is depicted in figure 3.9 .

$$F_n = 2T\sin\frac{\theta}{2(n+1)} \tag{23}$$

Thus,

$$F_1 = F_2 = F_n = 2T\sin\frac{\theta}{2(n+1)} = F \tag{24}$$

$$T = \frac{F}{2\sin\frac{\theta}{2(n+1)}} \tag{25}$$

Now using equation (22) and (24)

$$EIy = \sum_{i=1}^{n} +2T\sin\left(\frac{\theta}{2(n+1)}\right)\frac{\cos\phi_1}{6}(1+\tan^2\phi_1)[\langle x-a_1\rangle^3(L-a_1)^2(3x-2L-a_1)] - \frac{Te}{2}(x-L)^2 \tag{26}$$

At $x = 0$

$$EIy_{max} = \sum_{i=1}^{n} -2T\sin\frac{\theta}{2(n+1)}\frac{\cos\phi_1}{6}(1+\tan^2\phi_1)(L-a_1)^2(2L+a_1) - \frac{Te}{2}L^2 \tag{27}$$

Tension in the SMA wire is found to be

$$T = \frac{EIy_{max}}{\left[\sum_{i=1}^{n} -2\sin\frac{\theta}{2(n+1)}\frac{\cos\phi_1}{6}(1+\tan^2\phi_1)(L-a_1)^2(2L+a_1) - \frac{eL^2}{2}\right]} \tag{28}$$

where for the n th hook, angle with horizontal is (see figure 3.9)

$$\phi_1 = 1.\frac{\theta}{n+1}, \quad \phi_2 = 2.\frac{\theta}{n+1}$$

$$\phi_n = n.\frac{\theta}{n+1}$$

$$\phi_{n+1} = (n+1).\frac{\theta}{n+1} = \theta$$

3.4 SELECTION OF THE THREE-LINK ARM CONFIGURATION AND ITS WORK VOLUME

One of the most important parameter in designing of a robot

arm is to have a suitable work volume fulfilling the users requirements. Thus, selection of the three-link arm configuration is an important factor. Another important criterion in selection of the arm configuration is that forces transferred to the first link should not cause it to bend in its inactive state due to gravity effect. The configuration selected taking into account the above factors is shown in figure 3.3 .

Referring to the configuration of the three-link arm in the figure 3.3a,the link1 rotates about the y_0-axis and it is fixed vertically. The link2 rotates about the x_1-axis and is also fixed vertically but it is at 90^o to the link1. The link3 rotates about the x_2-axis and is fixed horizontally. It is at 90^o to both the other links. Thus, it can be seen that the rotation at link1 will give displacement to the arm end point in x_3 direction.Similarly the rotation of link2 will give displacement to the free end of the arm in y_3 direction and the rotation at link3 is for displacement in z_3 direction.

The position of the free end of the arm can be determined by post multiplying the transformation matrices of link1, link2 and link3 respectively.

Thus,

$$T_A = \text{Trans}[y, \frac{\theta_1}{2}].\text{Trans}[x, \frac{\theta_2}{2}].\text{Trans}[x, \frac{\theta_3}{2}]$$

where T_A = Resultant transformation matrix

$\text{Trans}[p, \frac{\theta_i}{2}]$ = Transformation matrix for link i, i = 1,2,3 about the p th axis.

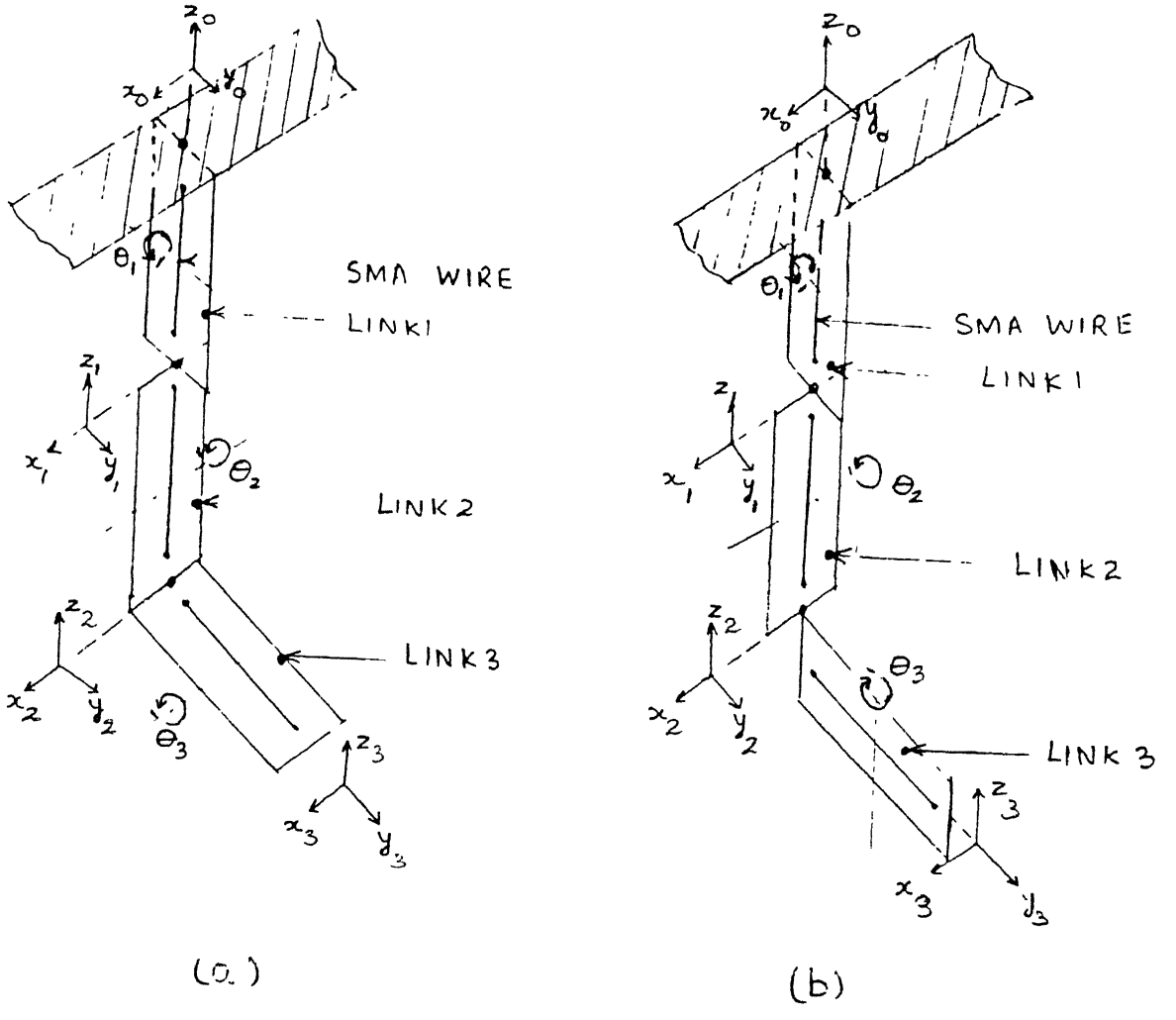

Figure 3.3 Schematic diagram of two arm configurations

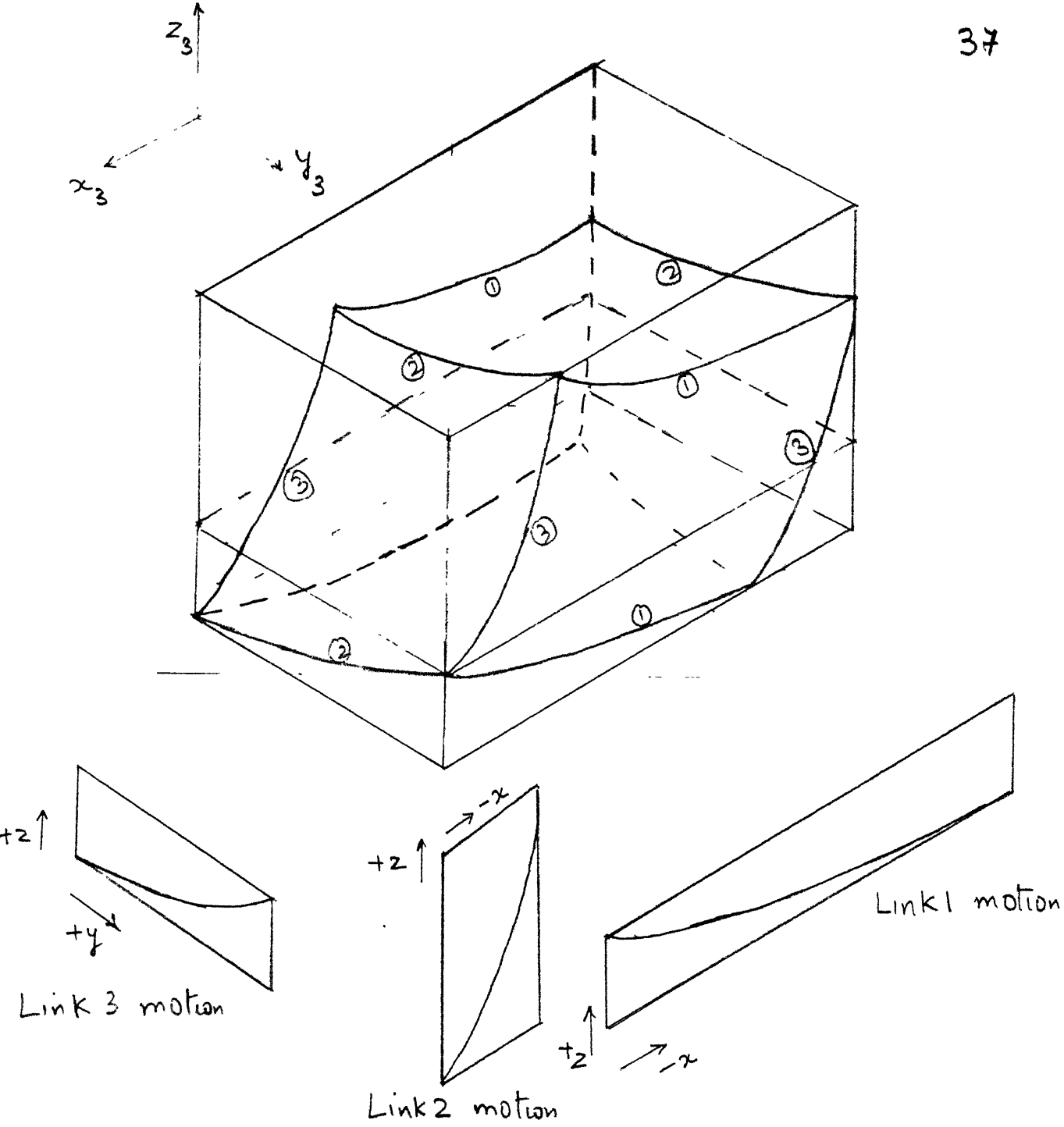

Figure 3.4 Schematic diagram of work volume

Now, to find the translations of the end point of the link caused by a Link rotating by $\frac{\theta}{2}$ radius as shown in figure 3.2 (small angle assumption is made) .

$R\theta = L$

$P = R(1 - \cos\theta) = R(1 - (1 - \frac{\theta^2}{2!})) = \frac{R\theta^2}{2} = \frac{L\theta}{2}.$

$P = \frac{L\theta}{2}$

$Q = R\sin\theta = R(\theta - \frac{\theta^3}{3!}) = \frac{L}{\theta}(\theta - \frac{\theta^3}{3!}) = L(1 - \frac{\theta^2}{6})$

$\frac{R_1}{2} = R\sin\frac{\theta}{2} = \frac{L}{\theta}(\frac{\theta}{2} - \frac{(\frac{\theta}{2})^3}{3!}) = \frac{L}{\theta}(\frac{\theta}{2} - \frac{\theta^3}{48}) = L(\frac{1}{2} - \frac{\theta^2}{48})$

$\Rightarrow \frac{R_1}{2} = \frac{L}{2}(1 - \frac{\theta^2}{24})$

$\Rightarrow R_1 = L(1 - \frac{\theta^2}{24})$

$R_1 \simeq L$

The transformation matrix is made of the rotation part and the translation part.As shown in the above figure 3.3a for the given rotation $\frac{\theta}{2}$ there is translation $P = \frac{L\theta}{2}$ and $Q = L(1 - \frac{\theta^2}{6})$ about two perpendicular axis with no translation in the third orthogonal axis.

Here C is for Cos and S is for Sin

Thus,

$$\text{Trans}[y_0, \frac{\theta_1}{2}] = \begin{bmatrix} C\frac{\theta_1}{2} & 0 & S\frac{\theta_1}{2} & \frac{-L\theta_1}{2} \\ 0 & 1 & 0 & 0 \\ -S\frac{\theta_1}{2} & 0 & C\frac{\theta_1}{2} & L(1-\frac{\theta_1^2}{6}) \\ 0 & 0 & 0 & 1 \end{bmatrix}$$

$$\text{Trans}\left[x_1, \frac{\theta_2}{2}\right] = \begin{bmatrix} 1 & 0 & 0 & 0 \\ 0 & C\frac{\theta_2}{2} & -S\frac{\theta_2}{2} & \frac{L\theta_2}{2} \\ 0 & S\frac{\theta_2}{2} & C\frac{\theta_2}{2} & L\left(1-\frac{\theta_2^2}{6}\right) \\ 0 & 0 & 0 & 1 \end{bmatrix}$$

$$\text{Trans}\left[x_2, \frac{\theta_3}{2}\right] = \begin{bmatrix} 1 & 0 & 0 & 0 \\ 0 & C\frac{\theta_3}{2} & -S\frac{\theta_3}{2} & -L\left(1-\frac{\theta_3^2}{6}\right) \\ 0 & S\frac{\theta_3}{2} & C\frac{\theta_3}{2} & \frac{L\theta_3}{2} \\ 0 & 0 & 0 & 1 \end{bmatrix}$$

$$T_A = \text{Trans}\left[y, \frac{\theta_1}{2}\right] \text{Trans}\left[x, \frac{\theta_2}{2}\right] \text{Trans}\left[x, \frac{\theta_3}{2}\right]$$

$$T_A = \begin{bmatrix} n_x & S_x & a_x & P_x \\ n_y & S_y & a_y & P_y \\ n_z & S_z & a_z & P_z \\ 0 & 0 & 0 & 1 \end{bmatrix}$$

$$n_x = C\frac{\theta_1}{2}, \quad n_y = 0, \quad n_2 = -S\frac{\theta_1}{2}$$

$$S_x = S\frac{\theta_1}{2}\, S\frac{\theta_2}{2}\, C\frac{\theta_3}{2} + S\frac{\theta_1}{2}\, C\frac{\theta_2}{2}\, S\frac{\theta_3}{2}$$

$$S_y = C\frac{\theta_2}{2}\, C\frac{\theta_3}{2} - S\frac{\theta_2}{2}\, S\frac{\theta_3}{2}$$

$$S_z = C\frac{\theta_1}{2}\, S\frac{\theta_2}{2}\, C\frac{\theta_3}{2} + C\frac{\theta_1}{2}\, C\frac{\theta_2}{2}\, S\frac{\theta_3}{2}$$

$$a_x = -S\frac{\theta_1}{2}\, S\frac{\theta_2}{2}\, S\frac{\theta_3}{2} + S\frac{\theta_1}{2}\, C\frac{\theta_2}{2}\, C\frac{\theta_3}{2}$$

$$a_y = - C\frac{\theta_2}{2}\, S\frac{\theta_3}{2} - S\frac{\theta_2}{2}\, C\frac{\theta_3}{2}$$

$$a_Z = - C\frac{\theta_1}{2}\, S\frac{\theta_2}{2}\, S\frac{\theta_3}{2} + C\frac{\theta_1}{2}\, C\frac{\theta_2}{2}\, C_2\frac{\theta_3}{2}$$

$$p_x = - S\frac{\theta_1}{2}\, S\frac{\theta_2}{2}\, L(1 - \frac{\theta_3^2}{6}) + S\frac{\theta_1}{2}\, C\frac{\theta_2}{2}\, \frac{L\theta_3}{2} + S\frac{\theta_1}{2}\, L(1 - \frac{\theta_2^2}{6}) - \frac{L\theta_1}{2}$$

$$p_y = - C\frac{\theta_2}{2}\, L(1 - \frac{\theta_3^2}{6}) - S\frac{\theta_2}{2}\, \frac{L\theta_3}{2} + \frac{L\theta_2}{2}$$

$$p_Z = - C\frac{\theta_1}{2}\, S\frac{\theta_2}{2}\, L(1 - \frac{\theta_3^2}{6}) + C\frac{\theta_1}{2}\, C\frac{\theta_2}{2}\, \frac{L\theta_3}{2} + C\frac{\theta_1}{2}\, L(1 - \frac{\theta_2^2}{6}) + L(1 - \frac{\theta_1^2}{6})$$

The position coordinates with the transformation matrix of the end point of the arm is given below as shown in figure 3.3b.

$$T_B = \text{Trans}[y, \tfrac{\theta_1}{2}].\text{Trans}[x, \tfrac{\theta_2}{2}].\text{Trans}[z, \tfrac{\theta_3}{2}]$$

$$P_x = C\frac{\theta_1}{2}\, \frac{L\theta_3}{2} - L\, S\frac{\theta_1}{2}\, S\frac{\theta_2}{2}\, (1 - \frac{\theta_3^2}{6}) + LS\frac{\theta_1}{2}\, (1 - \frac{\theta_2^2}{6}) - \frac{L\theta_1}{2}$$

$$P_y = - LC\frac{\theta_2}{2}\, (1 - \frac{\theta_3^2}{6}) + \frac{L\theta_2}{2}$$

$$P_Z = - S\frac{\theta_1}{2}\, \frac{L\theta_3}{2} - LC\frac{\theta_1}{2}\, S\frac{\theta_2}{2}\, (1 - \frac{\theta_3^2}{6}) + LC\frac{\theta_1}{2}(1 - \frac{\theta_2^2}{6}) + L(1 - \frac{\theta_1^2}{6})$$

For the other type of configuration as shown in the figure 3.3b where the last link has its rotation about the z axis , it can be seen that the control towards z position is lost. This happens because the link 3 rotates to give x position bringing redundancy in the configuration . Thus, this configuration is not used.

3.5 ANALYSIS FOR FORCE IN SMA WIRE FOR GIVEN STRAINS IN THE THREE LINKS OF THE ROBOT ARM

Referring to the figure 3.3a, the configuration shows that the arm consists of three links and to the end of the arm is attached the gripper. The links can be rotated in clockwise and anti clockwise direction.

The Link1 is rigidly fixed at one end and its other end is fixed to Link2. It rotates about the y axis to give displacement along the x axis. The Link 2 is further connected to Link3. It rotates about the x axis to give displacement along y axis. To the Link3 the griper is fixed and it is held to Link2. It rotates about the x axis to give displacement along z axis.

The tension in the SMA wire for any link can be found neglecting the effect of the SMA wire on the opposite side for that link.

Considering the forces acting on the Link3, which are uniform loading due to the weight of the Link and the weight of the gripper, the tension in SMA wire is found as follows:

Let

W = Weight of the Link

L = Length of the Link

I = Moment of Inertia of the Link

E = Modulus of Elasticity for Link Material

ε_j = Strain in SMA wire j = 1,2,3 for jth Link.

R_j = Radius of Curvature j = 1,2,3 for jth Link

D_j = Displacement of the free end of jth Link j = 1,2,3

w_j = Uniformly distributed load of jth Link j = 1,2,3

Wg = Weight of the gripper

e = Distance between SMA wire and the Link

Consider the Link 3.

$$w_3 = \frac{W}{L} \;,\; \theta_3 = \frac{\varepsilon_3 L}{e} \;,\; R_3 = \frac{e}{\varepsilon_3} \;,\; D_3 = \frac{e}{\varepsilon_3}(1 - \cos\theta_3)$$

Now, $EIy_{3T} = EI(y_{3w} + y_{3L} + y_G)$

where

y_{3T} = Total displacement of the free end of Link 3.

y_{3w} = Displacement of free Link end due to wire actuation

y_{3L} = Displacement of free Link end due to its own weight.

y_G = Displacement of free Link end due to weight of the gripper.

$$y_{3L} = \frac{wL^4}{8EI} = \frac{WL^3}{8EI} \qquad \text{and} \qquad y_G = \frac{W_g L^3}{3EI}$$

Using above equations and eq 27 of section 3.4 we get

$$EIy_{3T} \approx \sum_{i=}^{n} -2T_3 \frac{\theta}{2(n+1)} \frac{\cos\phi_1}{6} (1+\tan^2\phi_1)(L-a_1)^2(2L+a_1) - \frac{eL^2}{2} \pm \frac{WL^3}{8} \pm \frac{WL}{}$$

+/- (Down/Up) (1)

$$T_3 = \frac{EIy_{3T} \mp \frac{W_g L^3}{3} \mp \frac{WL^3}{g}}{\left[\sum_{i=1}^{n} -2\sin\frac{\theta_3}{2(n+1)} \frac{\cos\phi_{3i}}{6} (1+\tan^2\phi_{3i})(L-a_{3i})^2(2L+a_{3i}) - \frac{eL^2}{2}\right]} \qquad (2)$$

-/+ (Down/Up)

ow, $EI\frac{dy}{dx} = EI\left(\frac{dy_w}{dx} + \frac{dy_L}{dx} + \frac{dy_g}{dx}\right)$ (3)

$$\frac{dy_{3L}}{dx} = \frac{wL^3}{6EI} = \frac{WL^2}{6EI} \qquad (4)$$

$$\frac{dy_g}{dx} = \frac{WL^2}{2EI} \qquad (5)$$

Using equation 3.4.5 and equation13.15 of section 3.3

$$\theta'_3 = \left[\sum_{i=1}^{n} 2T_3 \sin\left(\frac{\theta}{2(n+1)}\right) \frac{\cos\phi_1}{EI} (1+\tan^2\phi_{3_1})(L-a_{3_1})^2 + \frac{T_3 eL}{EI} \right] \pm \frac{WgL}{2} + \frac{WL^2}{6} \quad (6)$$

The bending moment caused by the weight of link and the gripper is

$$M_3 = -\frac{WL^2}{2} - WgL = -L_3\left(\frac{W}{2} - Wg\right)$$

A counter balance has been placed to give the same magnitude of reverse bending moment as given by the weights of Link 3 and the gripper to ensure that Link1 and Link2 remain vertical.

The design of the counter balance is by equating the moment caused by the Link 3 and the gripper by the moment produced by the counter balance.

$$-\frac{w_c L_c^2}{2} = M_3$$

where $w_c = \rho_d \times L_c \times b_c \times t_c$

$$-\frac{W_c L_c}{2^2} = -L_3\left(\frac{W}{2} + Wg\right)$$

$$\frac{\rho_c L_c^2 b_c t_c}{2} = L_3\left(\frac{W}{2} + Wg\right)$$

$$t_c = \frac{2L_3\left(\frac{W}{2} + Wg\right)}{\rho_c L_c^2 t_c}$$

Thus, the thickness of the counter balance can be found given its length, breadth and density.

Considering the Link 2

$$w_2 \approx \frac{W}{D_2}, \quad \theta_2 = \frac{\varepsilon_2 L}{e}, \quad R_2 = \frac{e}{\varepsilon_2}, \quad D_2 = \frac{e}{\varepsilon_2}(1 - \cos\theta_2)$$

Now, $EIy_{2T} = EI(y_{2w} + y_{2L})$

where

y_{2T} = Total displacement of the free end of Link 2.

y_{2w} = Displacement of free Link2 end due to wire actuation

y_{2L} = Displacement of free Link2 end due to its own weight.

$$y_{2L} = \frac{w_2 D_2^4}{8EI} = \frac{WD_2^3}{8EI}$$

$$EIy_{2T} \approx \sum_{i=1}^{n} -2T_2 \sin\left(\frac{\theta}{2(n+1)}\right) \frac{\cos\phi_1}{6} (1+\tan^2\phi_{2i})(L-a_{2i})^2(2L+a_{2i}) - \frac{eL^2}{2} - \frac{W_2 D}{8} \quad (7$$

$$T_2 = \frac{EIy_{2T} - \frac{W_2 D_2^3}{8}}{\left[\sum_{i=}^{n} -2\sin\frac{\theta_2}{2(n+1)} \frac{\cos\phi_{2i}}{6} (1+\tan^2\phi_{2i})(L-a_{2i})^2(2L+a_{2i}) - \frac{eL^2}{2}\right]} \quad (8)$$

$$\frac{dy_{2L}}{dx} = \frac{w_2 D_2^3}{6EI} = \frac{WD_2^2}{6EI}$$

Similarly,

$$\theta'_2 = \left[\sum_{i=1}^{n} 2T_2 \sin\left(\frac{\theta}{2(n+1)}\right) \frac{\cos\phi_{2i}}{EI} (1+\tan^2\phi_{2i})(L-a_{2i})^2 + \frac{T_2 eL}{EI}\right] - \frac{WD_2^2}{6EI} \quad (9)$$

Considering the Link 1

$$w_1 \approx \frac{W}{D_1}, \quad \theta_1 = \frac{\varepsilon_1 L}{e}, \quad R_1 = \frac{e}{\varepsilon_1}, \quad D_1 = \frac{e}{\varepsilon_1}(1 - \cos\theta_1)$$

Now,

$$EIy_{1T} = EI(y_{1w} + y_{1L})$$

where

y_{1T} = Total displacement of the free end of Link1

y_{1w} = Displacement of the free Link1 end due to wire actuation

y_{1L} = Displacement of the free Link1 end due to its own weight.

$$T_1 = \frac{EIy_{1T} - \frac{W_1 D_1^3}{g}}{\left[\sum_{i=1}^{n} -2\sin\frac{\theta_1}{2(n+1)} \frac{\cos\phi_{1i}}{6} (1+\tan^2\phi_{1i})(L-a_{1i})^2(2L+a_{1i}) - \frac{eL^2}{2}\right]} \quad (10$$

Similarly,

$$\theta'_1 = \left[\sum_{i=1}^{n} 2T_1 \sin\left(\frac{\theta}{2(n+1)}\right) \frac{\cos\phi_{11}}{EI} (1+\tan^2\phi_{11})(L-a_{11})^2 + \frac{T_1 eL}{EI} \right] - \frac{WD_1^2}{6EI} \quad (11$$

3.6 METHOD OF FABRICATING THE STEEL LINK

The steel link was fabricated from a spring steel plate cut to the dimensions as shown in the figure 3.8. The Nitinol wire cannot be directly hooked to the steel link for the requirement of electrical insulation. This was because current would flow through the wire. The beads were made of bakelite and these were clamped to the link by hooks . The wire passed through these hooks. The screw to hold the wire at the ends also has to be insulated. Thus, a bakelite externally stepped hollow cylinder and a ring were manufactured and screw fixed to the link through them. The wire passed through the holes drilled in the screw and clamped at the ends by stoppers. See Appendix Cfor the steel link specifications.

To find the amount of bending of the link, Two metal wire strain gages were fixed on the link as shown in the figure3.8 one opposite the other. The strain gages were of 350 Ω resistance and gage factor of 2 . The strain gages were fixed opposite to each other so that the millivolt output was doubled and temperature compensation was also obtained. The strain gages were thermally insulated from the heated wire by Teflon sheet(0.2mm thick).

To find the temperature of both wires on both sides of the link reached on passing current, a Chromel- Alumel thermocouple was fixed on the wire by Sauercisen electrical cement. This cement

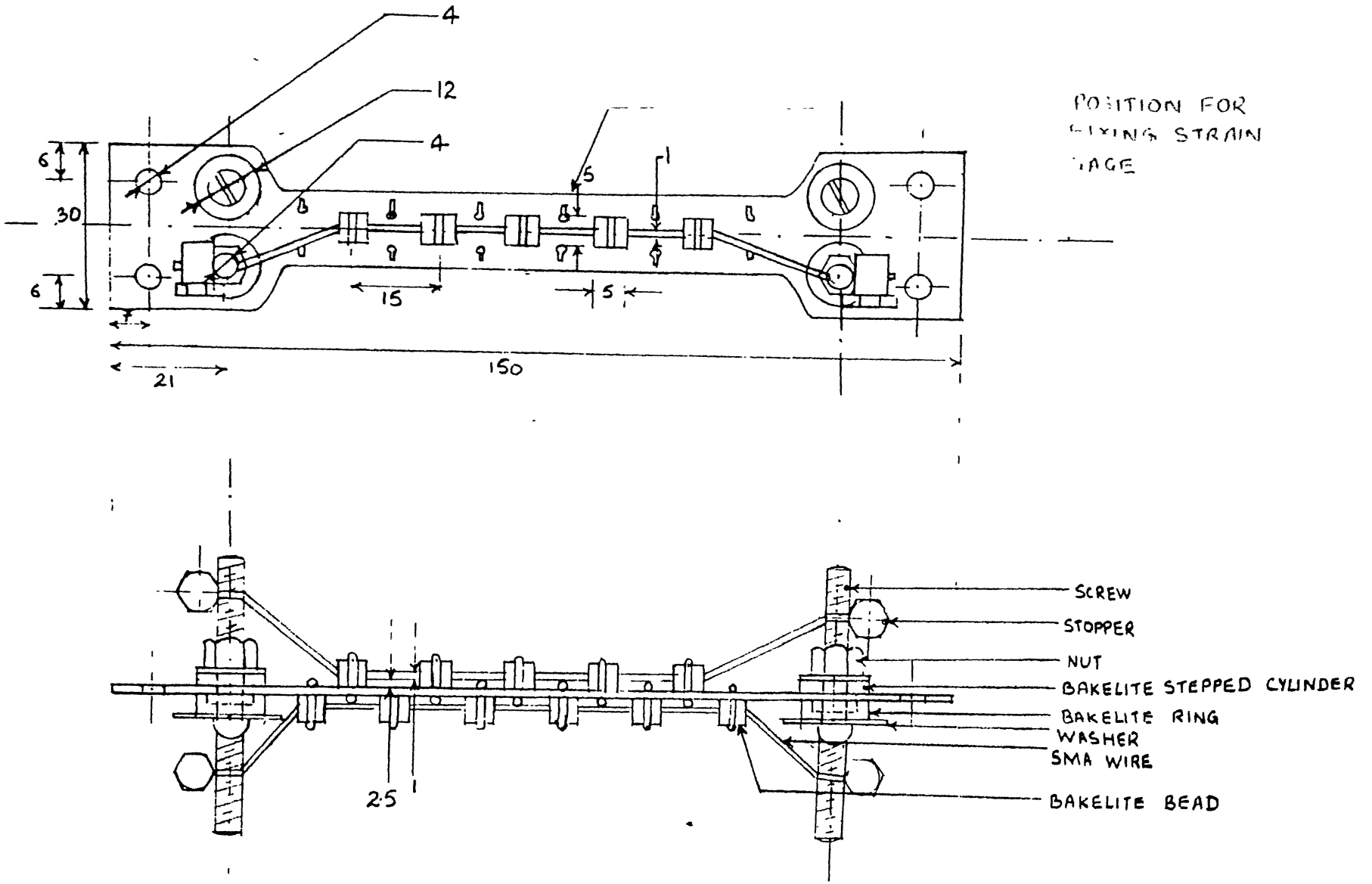

Figure 3.8 Steel link actuated by Nitinol wire

is an electrical insulator and thermal conductor. The method of fixing thermocouple hot junction to the wire was to prepare a paste of this cement with water and place the paste on the wire and thermocouple bead kept overlapping. The cement was baked for one hour at 60 - 70 C.

3.7 METHOD OF FABRICATING THE COMPOSITE LINK

The materials required in the fabrication of this type of link was a composite plate , actuator wire, hooks and mechanical fasteners. The composite used is E- Glass Epoxy. Two types of links were made from the above composite material. one with Nitinol as actuator and the other with biometal as actuator.

The composite plate was prepared in two sizes one with 1mm and the other with 0.5mm thickness. In the case of 1mm thick plate 6 laminates were used and for 0.5 mm thick plate 3 laminates were used. The method of making composite plates was that the laminates were piled one on top of each other and kept in a hot press for 30 minutes at a temperature of 150^{o}C and pressure of 30 kgf/cm^{2}. Then the temperature was made 80^{o}C and pressure increased ~~increased~~ to 65kgf/cm^{2}.For this changed heating cycle the laminates were kept for 2 hours.

The composite link with Nitinol as actuator was fabricated with the composite plate of size 150 *30 * 1 mm. In this holes were drilled for fixing of hooks and for fixing of the screw. The wire was passed through the hooks and hole in the screws and clamped by stoppers.

The composite link with biometal as actuator was fabricated with the composite plate of size 110* 15* 0.5 mm. In this case a hook made of composite plate was fitted and wire clamped at the ends .

3.8 MECHANICAL DESIGN OF THE GRIPPER

The Biometal wire actuated gripper having two jaws has been designed. It has been fabricated to carry light loads only. The use of more numbers of biometal wires can enhance the load carrying capacity of the gripper. As has been explained earlier the actuation of the bimetal wire occurs on its being heated i.e. it contracts applying a force on the body resisting its contraction. The schematic diagram for the half side of the gripper is shown in figure 3.10 The wire ends were kept near the hinge so that more deflection can be produced even though tension in wire would increase (see figure 3.11).

Considering the left half of the gripper only. The maximum contraction of the biometal wire is given by

$\delta_m = \frac{1}{2} \times$ Length of biometal wire x strain (max).

where, δ_m = maximum contraction.

The max angular rotation achieved by the jaw neglecting all forces resisting the biometal wire is given by

$\Delta\theta = \frac{\delta_m}{R_1}$ and $\theta_f = \theta_1 + \Delta\theta$

where, $\Delta\theta$ = Change in jaw angle

θ_1 = Initial jaw angle. θ_f = Final jaw angle.

R_1 = Length between hinge and the end of biometal wire.

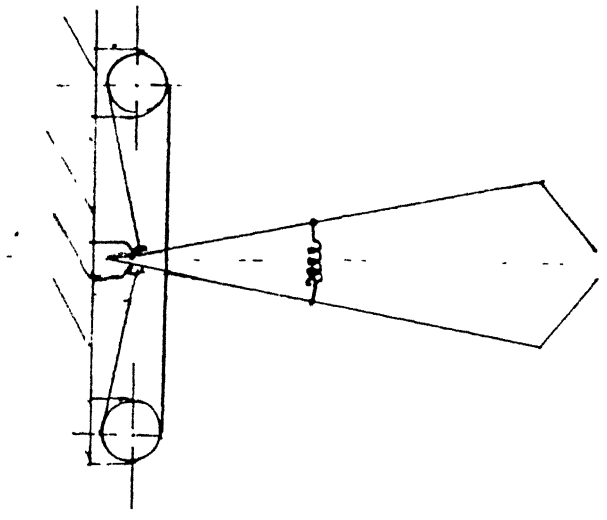

Figure 3.9 Schematic diagram of gripper

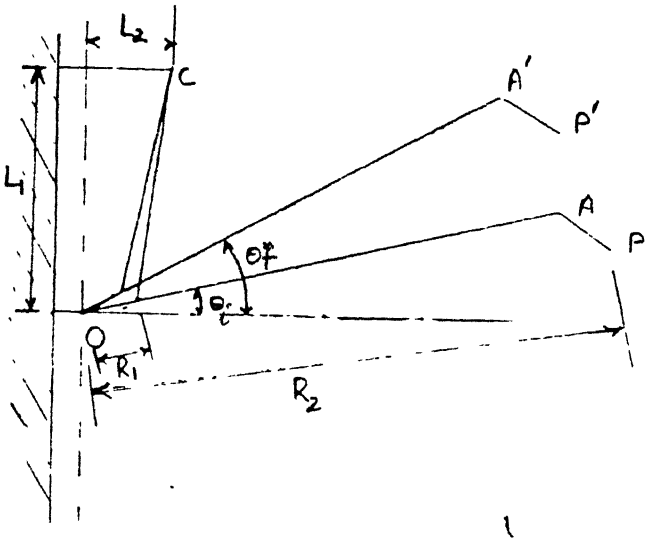

Figure 3.10 Schematic diagram of the jaw motion

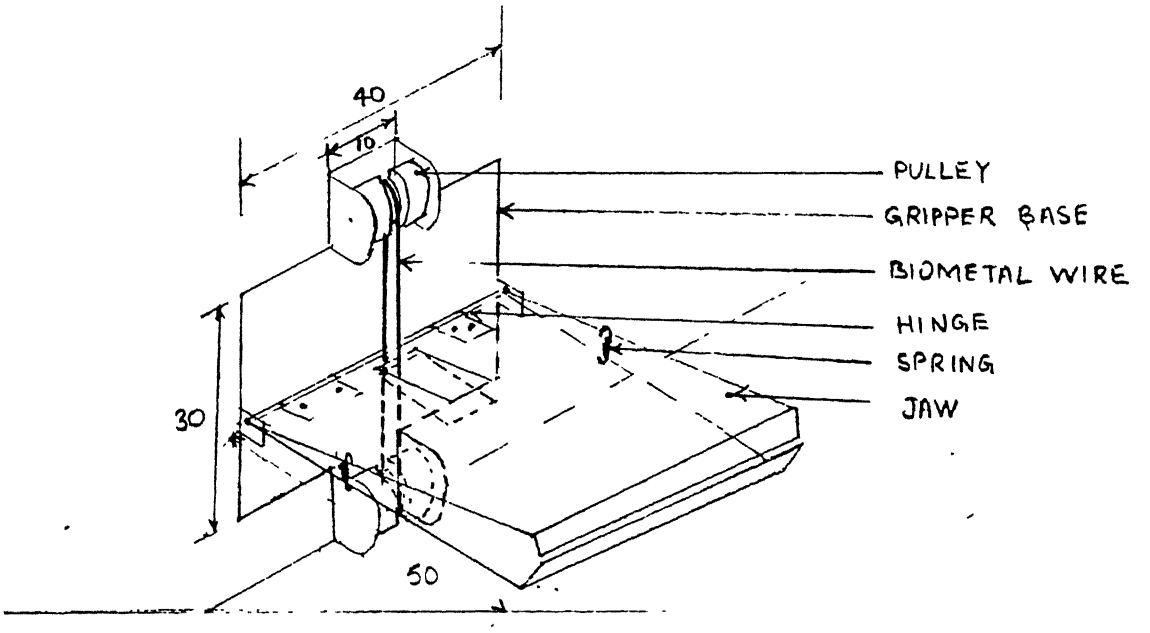

Figure 3.11 Gripper actuated by Biometal wire

The maximum displacement of the jaw end neglecting all resulting forces on biometal wire can be found by

$$\Delta\theta = \frac{\delta_m}{R_1} = \frac{d_m}{R_2}$$

$$d_m = \frac{R_2 \delta_m}{R_1}$$

where,

R_2 = Length between hinge and the outer end of the jaw.

d_m = Max displacement of outer end of the jaw from the initial position.

The maximum force acting on the biometal wire with the horizontal gripper axis can be found by equating the bending moments about the jaw hinge as shown in the figure 3.10.

$$T \sin\theta_f' . R_1 \cos\theta_f = F_s L_s \cos\theta_1 + \frac{mg(OA+AP)}{2} \sin\theta_f$$

$$T = (F_s L_s \cos\theta_1 + \frac{mg(OA+AP)}{2} \sin\theta_f) / R_1 \sin\theta_f' . \cos\theta_f)$$

The gripper was fabricated using an Aluminum base to keep the weight of gripper low(see also Appendix D). The Aluminum plate 1mm thick was bent to the required shape so that pulleys and jaws could be hinged to it. The pulleys were made of bakelite so that the wire was insulated from the base. The jaws were made from perspex and hinge fixed on it. The biometal wire was bolted at the ends to the jaws as shown in the figure 3.11. It was passed through one fixed and the other adjustable pulley so that the initial tension in the wire could be produced. A slot in the jaw was made so that the wire could be fixed on the side of the jaws.

CHAPTER IV

ELECTRICAL CONTROLS

4.1 CONTROL CIRCUIT DESCRIPTION

An effort had been made in electrically controlling the robot arm. The SMA wire required a given current so that the link can be desirably rotated. This variable current was to be controlled by the desired circuit as shown in the figure 4.1 and described below.

The approach in controlling was to create a duty cycle in the PC which would be an input to this circuit. A maximum permissible value of voltage was always across the wire with the power transistor (T2) also in between the supply and ground. This would mean that when transistor T2 is conducting, maximum current is flowing through the SMA wire. If in the other case the transistor T2 was not conducting then there would be no flow of current in the SMA wire. Thus, a duty cycle of ON and OFF time can be produced to give an output of required average current. This constant current would flow through the wire.

From the PCL 712 card, the digital output line was connected to the base of transistor T1; when this line went high (logic 1) the transistor T1 went in saturation mode. With this the transistor T2 went into cut-off. Thus, no flow of current through the SMA wire.

But, when the base of transistor T1 was low (logic 0), it went into cut-off mode and made transistor T2 go into saturation.

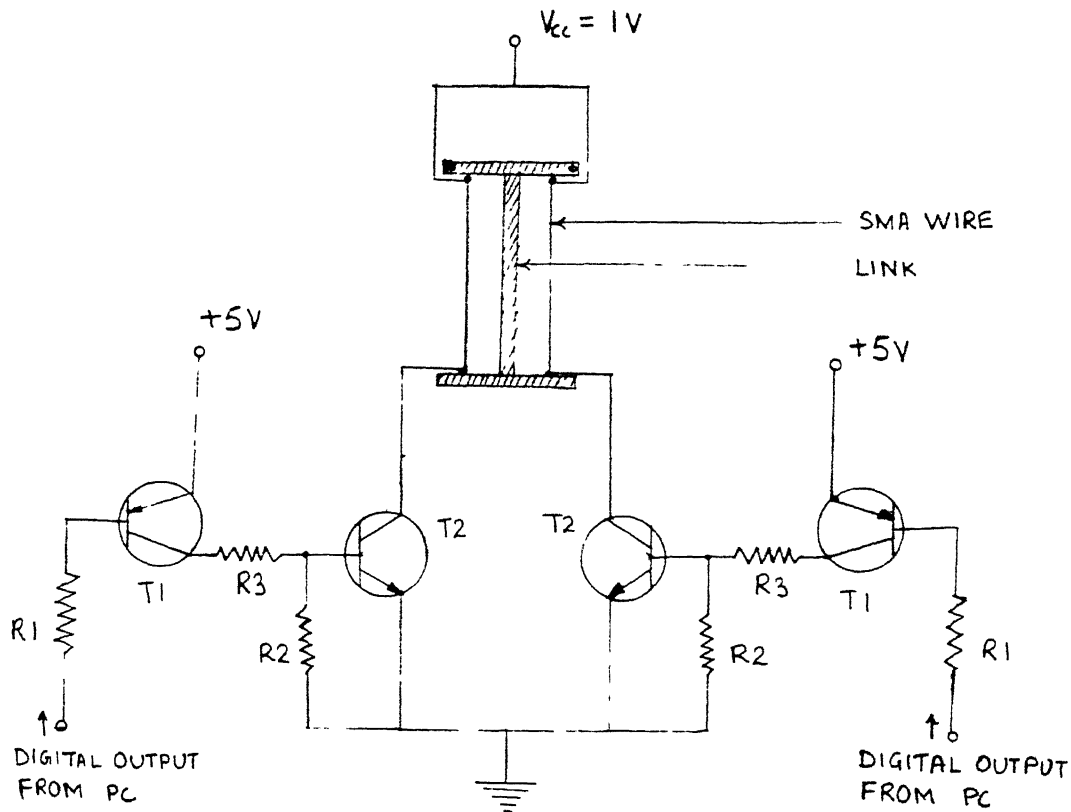

T1 = SK100
T2 = ECN055
R1 = 1kΩ, 1/4W
R2 = 1kΩ, 1/4W
R3 = 27Ω, 1W

Figure 4.1 : Control circuit for single link

The transistor T2 started conducting and max current flowed through the SMA wire heating it.

PCL 712 card allows maximum of 5 mA to flow through the digital output line in sink mode at 0.5 V (logic 0). Thus, a resistance (R1) of 1 kΩ was put in series to limit the above mentioned level of current

A resistance (R2) of 1 kΩ was placed across collector and base of transistor T2 so that when T2 went from saturation to cut-off the stored charge in T2 can be depleted out fast giving a faster switching

4.2 COMPUTER CONTROL ALGORITHM

As had been mentioned earlier the requirement of the duty cycle for proper position control of robot arm was required. The duty cycle would be produced in proportion to the current requirement for that link which itself is governed by the amount of displacements required to reach the given position.

The control algorithm is described below.

1) Input of required position (X,Y,Z)

   This is to be fed interactively to the personal computer.

2) To calculate current[1], current[2] and current[3] to be supplied to the three links by inverse kinematics.

3) Each link on being actuated by supplying current will give displacement in only two coordinate directions. This is shown in figure 5.18,5.19 and 5.20. It can be seen that link1

actuation gives displacement in x and z direction, link2 actuation gives displacement in y and z direction and finally link3 actuation gives displacement in z and y directions. To find the currents in the three links a set of simultaneous equations have to be solved which are stated below.

$$x = x[1]$$

$$y = y[2] + y[3]$$

$$z = z[1] + z[2] + z[3]$$

where x[i] = Displacement in x direction by ith link, i = 1,2,3.

y[i] = Displacement in y direction by ith link, i = 1,2,3.

z[i] = Displacement in z direction by ith link, i = 1,2,3.

But, it is evident from the figure 5.18, 5.19 and 5.20 that

i) Link1 prominently has displacement in x direction

ii) Link2 prominently has displacement y and z direction

iii) Link3 prominently has displacement z direction

Therefore this fact is used to decouple the above set of equations and an approximate procedure is followed i.e determine the current[1] in link1 for required x displacement. Then for required y displacement the current[2] is calculated , then the z displacement due to link1 and link2 is calculated. If required z displacement is more than this value then current[3] is calculated otherwise z position has been crossed. The figure 5.18, 5.19, 5.20 show the displacement versus current for the three links on being individually

actuated. By the linear interpolation in between the two adjoining data points about the required position the currents are calculated . The table 5.3 gives the linearly interpolated currents in the links for the required input position. To find the accuracy the position reached by end point is observed.

3) Calculate for a given time period (T) the OFF time for each link (t1, t2, t3) proportional to the current for that link so that the duty cycle can be produced.

4) Find the least, middle and highest OFF time from the three off times found in the above step.

5) Give appropriate digital output with all lines low.

6) Give a delay of the order of least OFF time.

7) Make the line with least OFF time high and keep remaining lines low. Give the appropriate digital output.

8) Give a delay of the order of (middle - least) OFF time.

9) Make the line corresponding to middle OFF time also high and keep highest OFF time line low. Give the appropriate digital output.

10) Give a delay of the order of (highest - middle) OFF time.

11) Make all lines high and give corresponding digital output.

12) Give a delay of (time period -highest) OFF time.

13) Repeat from step 5.

This algorithm gives three digital output pulses simultaneously so that the three links could be properly controlled to reach the required position.

CHAPTER V

EXPERIMENTAL RESULTS AND DISCUSSION

5.1 INTRODUCTION

In this chapter the results of experiments conducted have been presented and then discussed. The test were conducted on Nitinol and Biometal wire. Later, they were fixed on steel and composite links and their displacements observed for input currents. The rate of temperature rise of the Nitinol wire was also found by using thermocouples.

5.2 LOAD VS STRAIN TEST FOR SMA WIRE

This test is conducted on the SMA wire after it had been put to 25 cycles of heating and cooling under no load condition. After this the SMA wire is heated so that it reaches its minimum contracted position. Then the affect of different magnitudes of force on straining of the SMA wire were found. The method adopted for this test was as follows:

(1) Heat the wire at no load to its minimum position and then allow it to cool to room temperature. Note its length.

(2) Apply the required load and then after three minutes note the maximum length achieved.

(3) With load remaining applied, heat the wire by current of 4.0 Ampere and note the length achieved.

(4) Repeat step 2 and step 3 with increasing load in the steps of 1 Kg from no load till 17 Kg.

(5) Repeat step 2 and step 3 with decreasing load in the steps of 1 Kg from 17 Kg till no load.

LOAD (Kg)	AVAILABLE PERCENT STRAIN	UNAVAILABLE STRAIN DUE TO LOAD	PERCENT STRAIN
Ø	Ø	Ø	Ø
1	Ø	Ø	Ø
2	Ø.ØE	Ø	Ø.ØE
3	Ø.39	Ø	Ø.39
4	Ø.47	Ø	Ø.47
5	Ø.78	Ø	Ø.7E
6	Ø.86	Ø	Ø.86
7	1.Ø9	Ø	1.Ø9
8	1.25	Ø.16	1.41
9	1.33	Ø.16	1.49
10	1.4E	Ø.2E	1.7E
11	1.9E	Ø.2E	2.1E
12	1.9E	Ø.3E	2.2E
13	2.35	Ø.3E	2.66
14	2.66	Ø.3E	2.97
15	2.97	Ø.31	3.2E
16	3.1E	Ø.39	3.5E
17	3.2E	Ø.3E	3.6E

Table 5.1

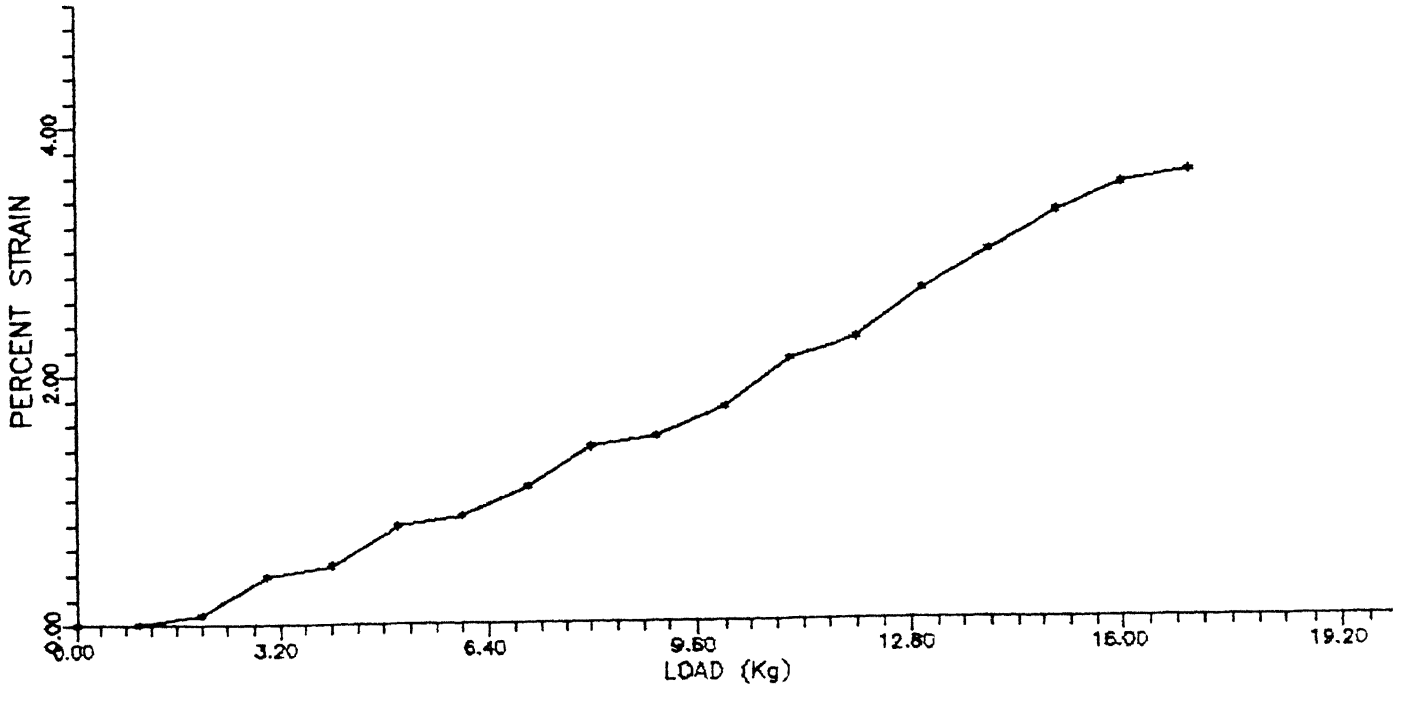

Fig. 5.1 Characteristics of Nitinol (SMA) wire

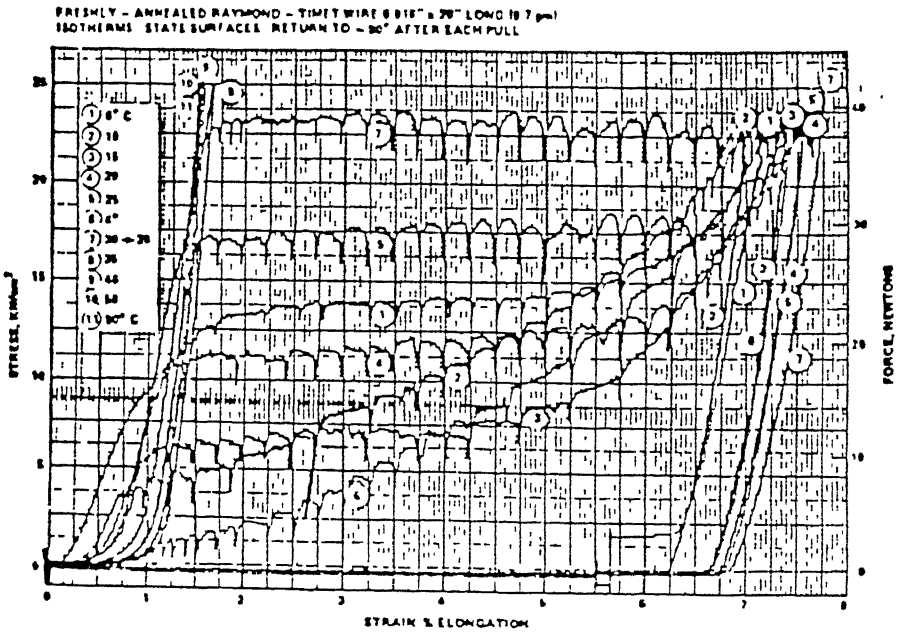

Figure 5.2 Characteristics of Nitinol wire (manufacturer Specification)

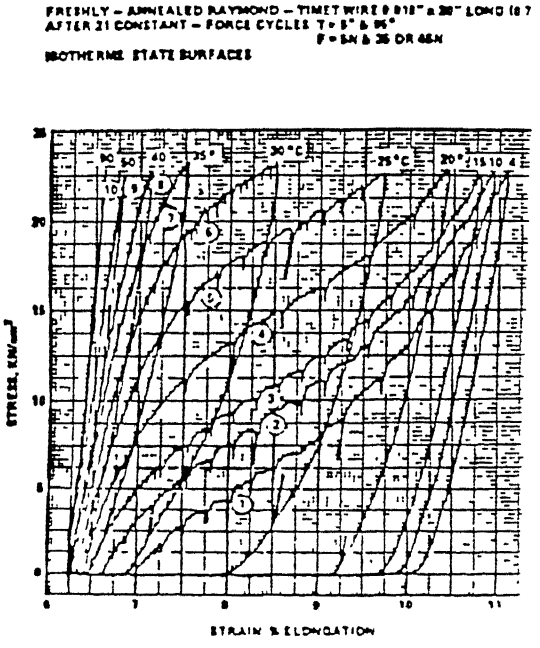

Figure 5.3 Characteristics of Nitinol wire (manufacturer specification)

This test matches with the figure 5.2 given by the manufacturers. There was a slight difference in both the graphs i.e. the figure 5.1 shows that there is elongation with increasing load. And, there is no region where for given stress value elongation would occur without any increase in load, but the figure 5.2 given by the manufacturer shows the latter. Furthermore, the amount of elongation achieved for a given load is lesser than the claim of the manufacturers for the given temperature.

5.3 LOAD VS STRAIN FOR BIOMETAL WIRE

In this case the experiment was similarly performed as done for the SMA wire.The only difference between the two was that here the increments and decrements were in steps of 20 gm and the maximum load applied was 200 gm.

The test here shows that till a certain load (170 gm)there is no elongation other than the available reversible shape memory effect(see figure 5.4). After increasing the load further the specimen gets elastic martensitic strain till a load of 200 gm and near the range of 350 gm the specimen went into permanent plastic deformation . At this stage the reversible SME is considerably lost.

The results obtained from the experiment conducted on Biometal wire shows that the material is ferroelastic i.e. it contracts on heating and elongates on cooling. The material is in the martensitic state at room temperature. About 4% of reversion stress is obtained fora load of less than 200 gm. The

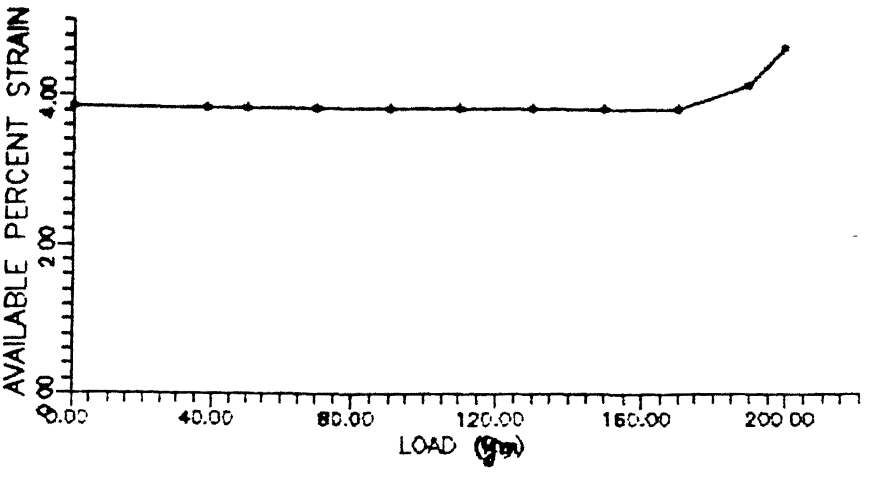

Fig. 5.4 Characteristics of Biometal (SMA) wire

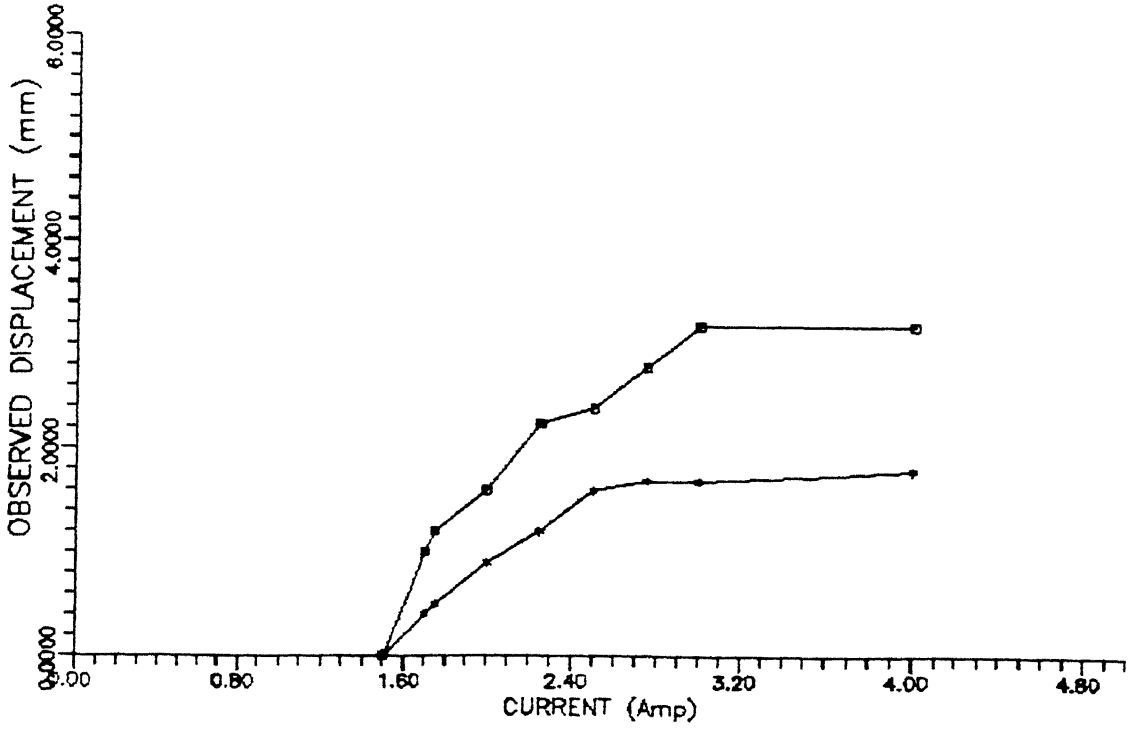

Fig.5.5 Characteristics of the steel link with SMA wire at 3% prestrain

manufacturer states that wire can take 3N of load but the wire on application of this much stress got plastically deformed and lost its trained behaviour.

5.4 DISPLACEMENT VS TIME AND TEMPERATURE VS TIME FOR DIFFERENT CURRENTS FOR STEEL LINK WITH NITINOL WIRE AT 3% PRESTRAIN

In this test two metal wire strain gages were fixed on the link(see figure 5.5), so that when the link bends one side goes into tension and the other into compression.These were insulated from heat of the wire by a teflon sheet.

The experiment was performed by firstly heating one side of the wire while the other was in the cooled state. The change in position of the free end of the link and increase in temperature of the wire was plotted by an omniscribe recorder. Observations of movement were also taken by a travelling microscope.

From the test it was observed that as the current increases the amount of movement also increases till a critical value of current (3.0 amp). .There is also an increase in the rate of change of position. It was also shown from the temperature vs time curve that the rate of temperature rise is approximately following an exponential curve.

When the current was switched off, it was observed that the free end of the link came back to its initial position by a great extent. The graph shows that the motion is very slow. The temperature vs time curve shows an approximately exponential decay curve(see figure 5.6 to 5.14).

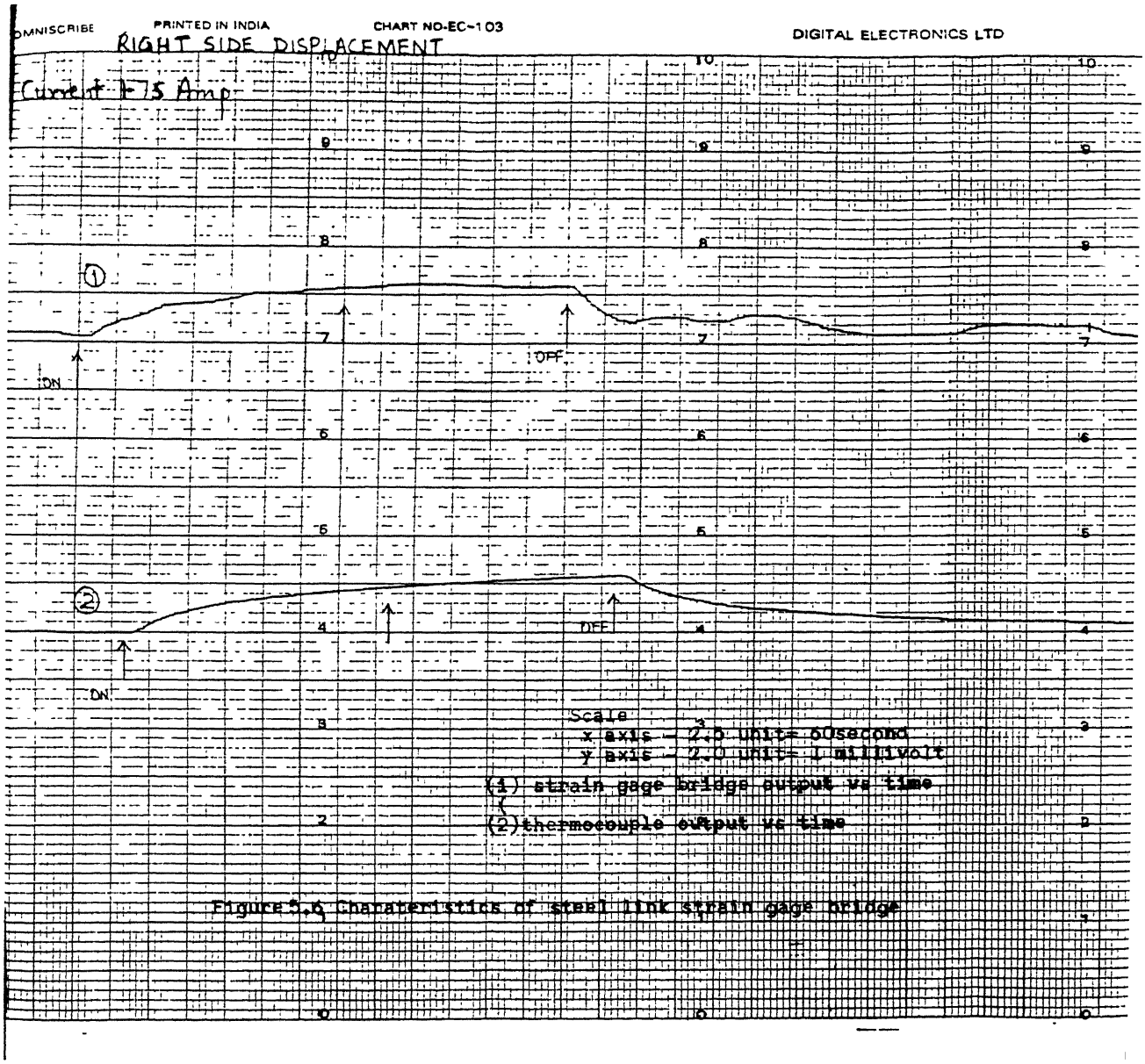

Figure 5.6 Characteristics of steel link strain gage bridge

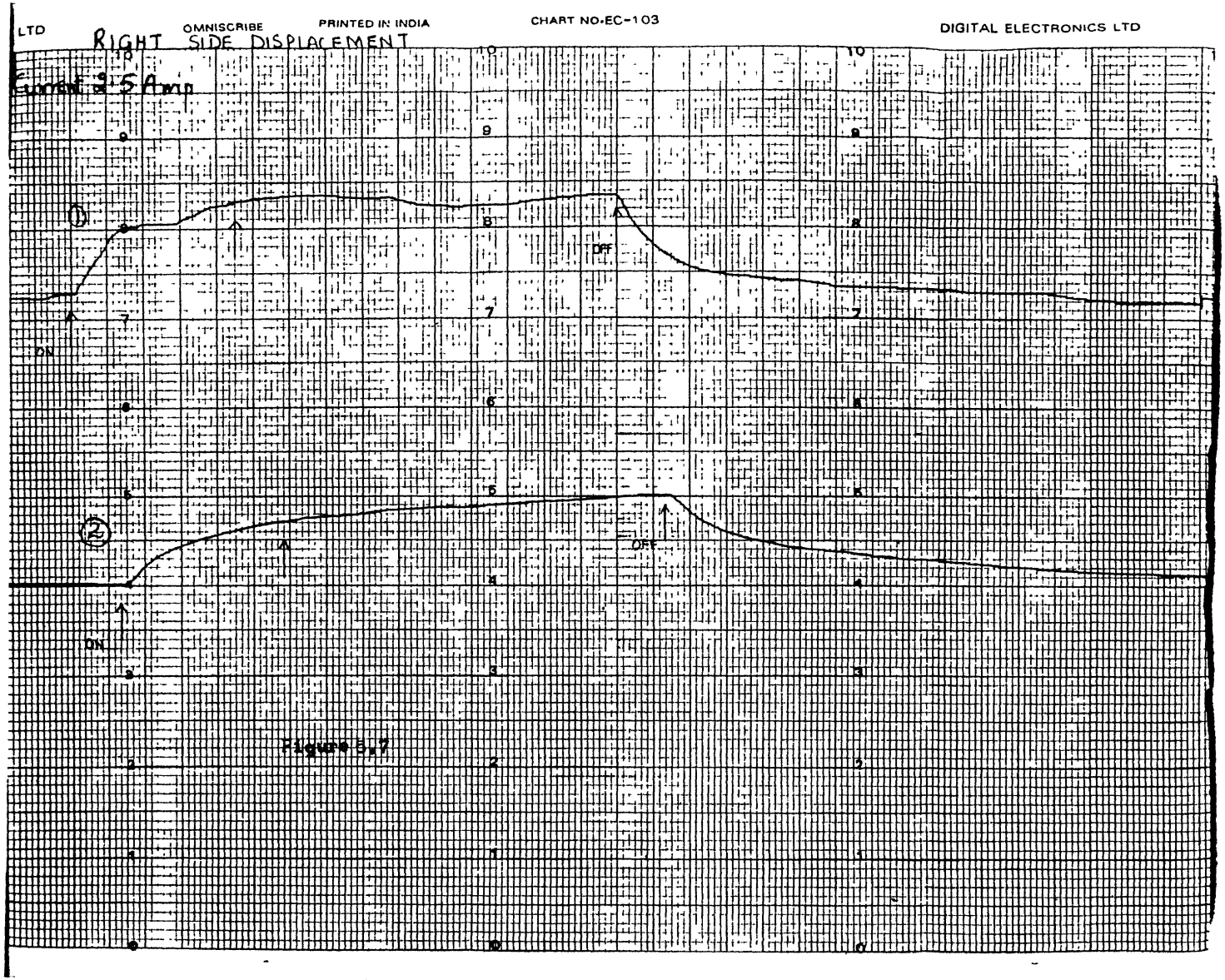
LTD
OMNISCRIBE
PRINTED IN INDIA
CHART NO-EC-103
DIGITAL ELECTRONICS LTD
RIGHT SIDE DISPLACEMENT
Current = 5 Amp
ON
OFF
ON
OFF

Figure 5.7

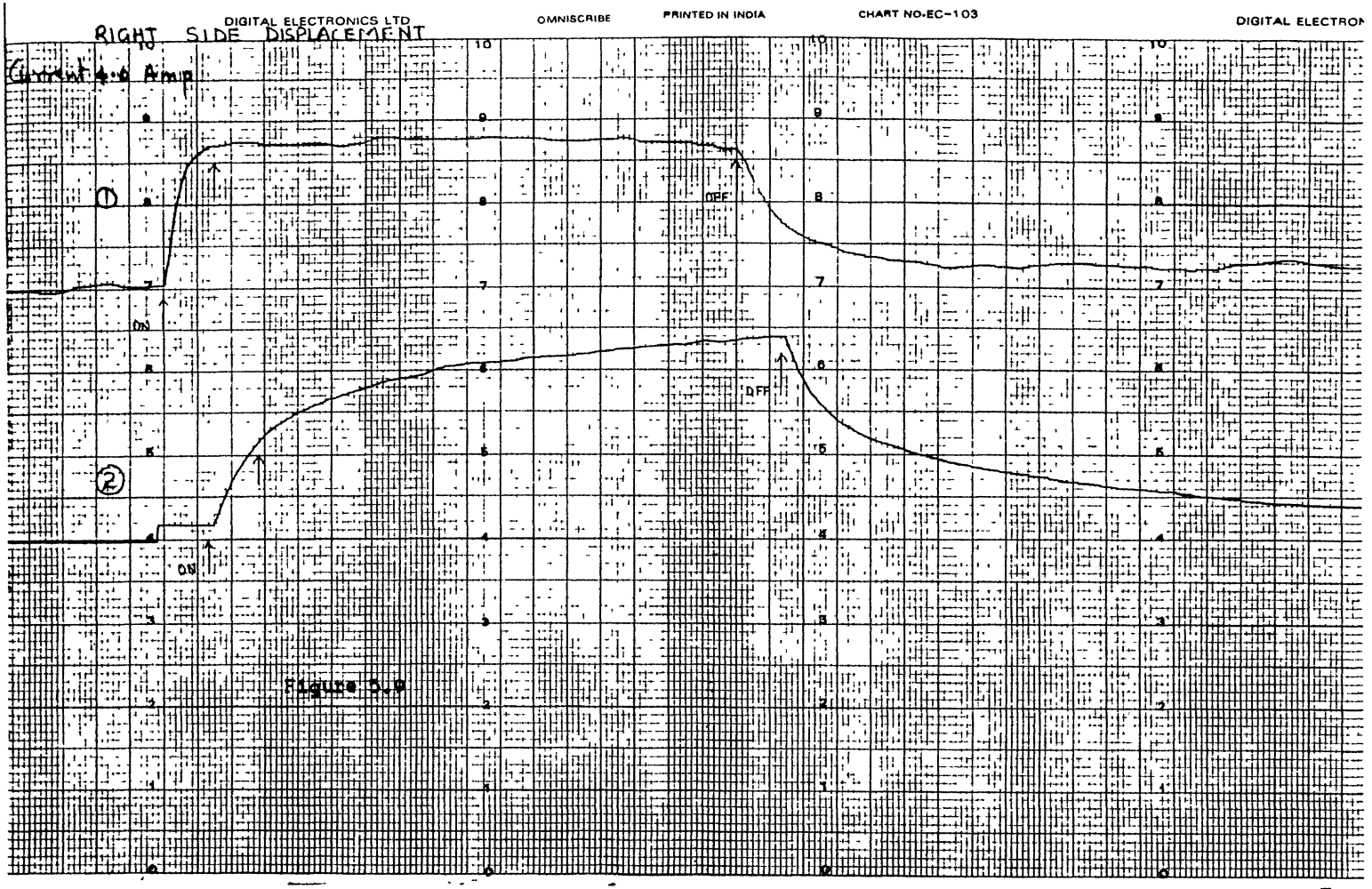
DIGITAL ELECTRONICS LTD
OMNISCRIBE
PRINTED IN INDIA
CHART NO-EC-103
DIGITAL ELECTRON
RIGHT SIDE DISPLACEMENT
Current 4.0 Amp
ON
OFF
ON
OFF

Figure 5.9

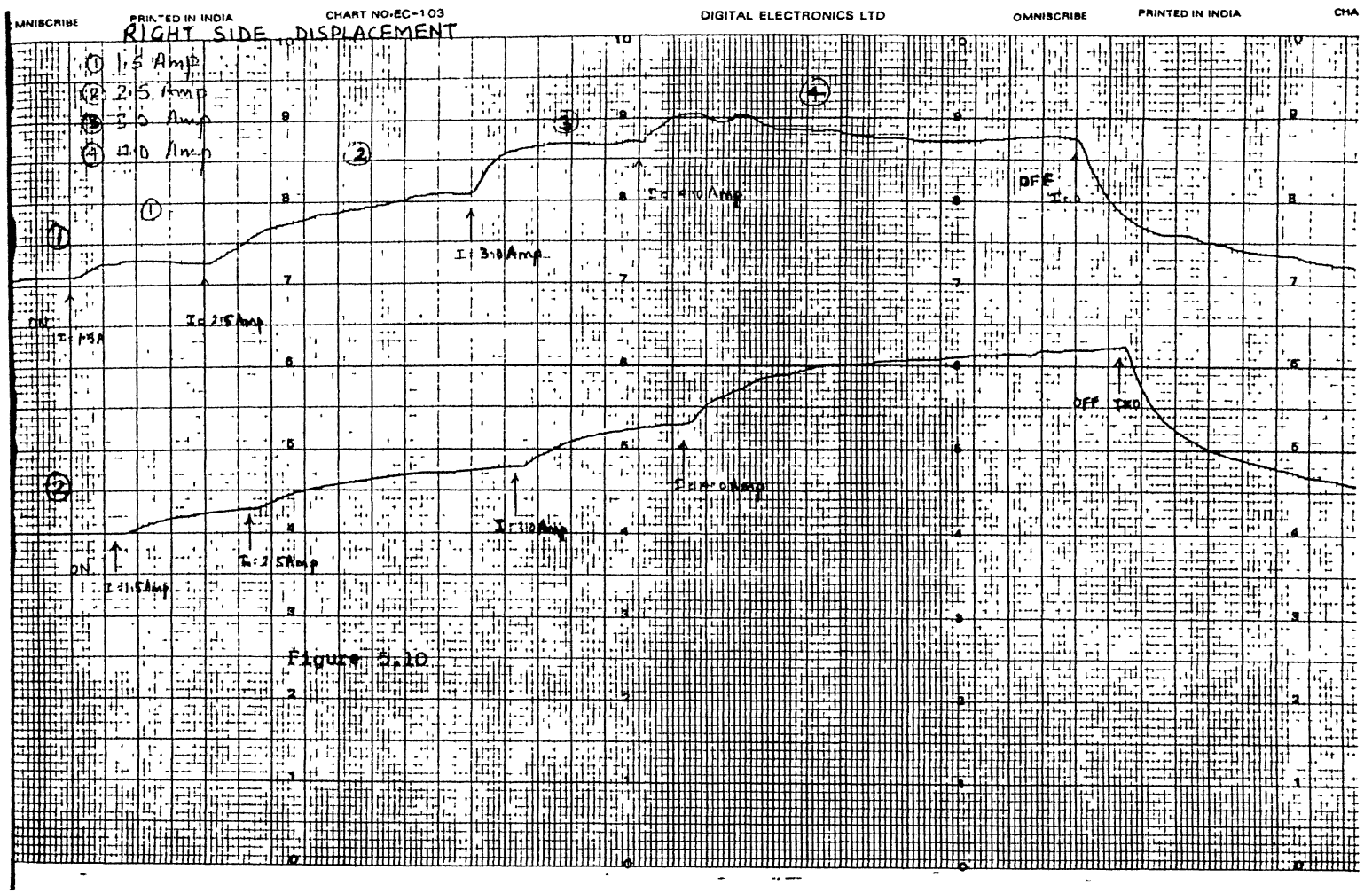
OMNISCRIBE PRINTED IN INDIA CHART NO.EC-103 DIGITAL ELECTRONICS LTD OMNISCRIBE PRINTED IN INDIA CHA
RIGHT SIDE DISPLACEMENT
① 1.5 Amp
② 2.5 Amp
③ 3.0 Amp
④ 4.0 Amp
I = 3.8 Amp
I = 4.0 Amp
OFF
I = 2.5 Amp
I = 1.5 A
ON
I = 3.0 Amp
OFF
I = 2.5 Amp
I = 1.5 Amp
ON

Figure 5.10

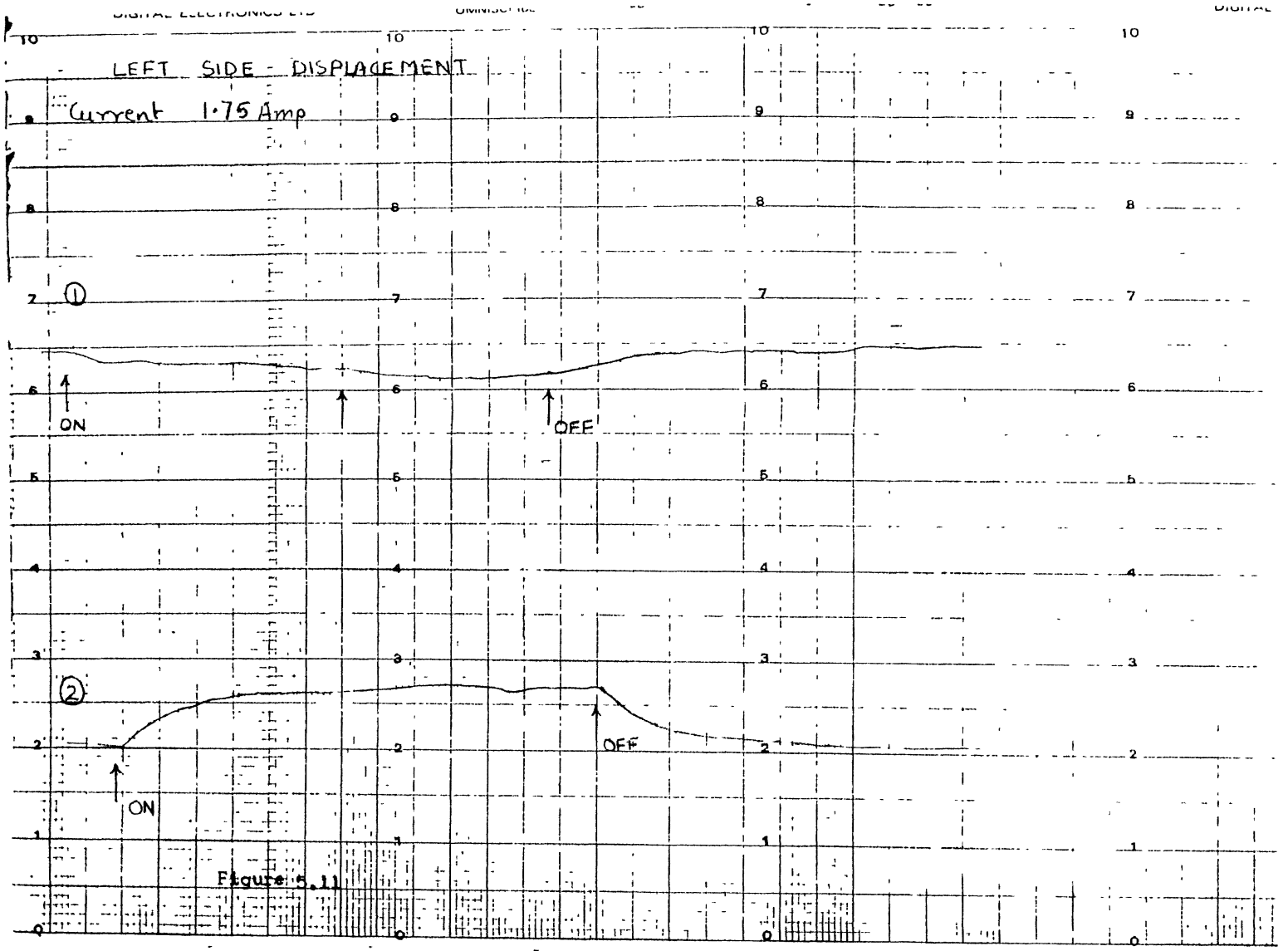

Figure 5.11

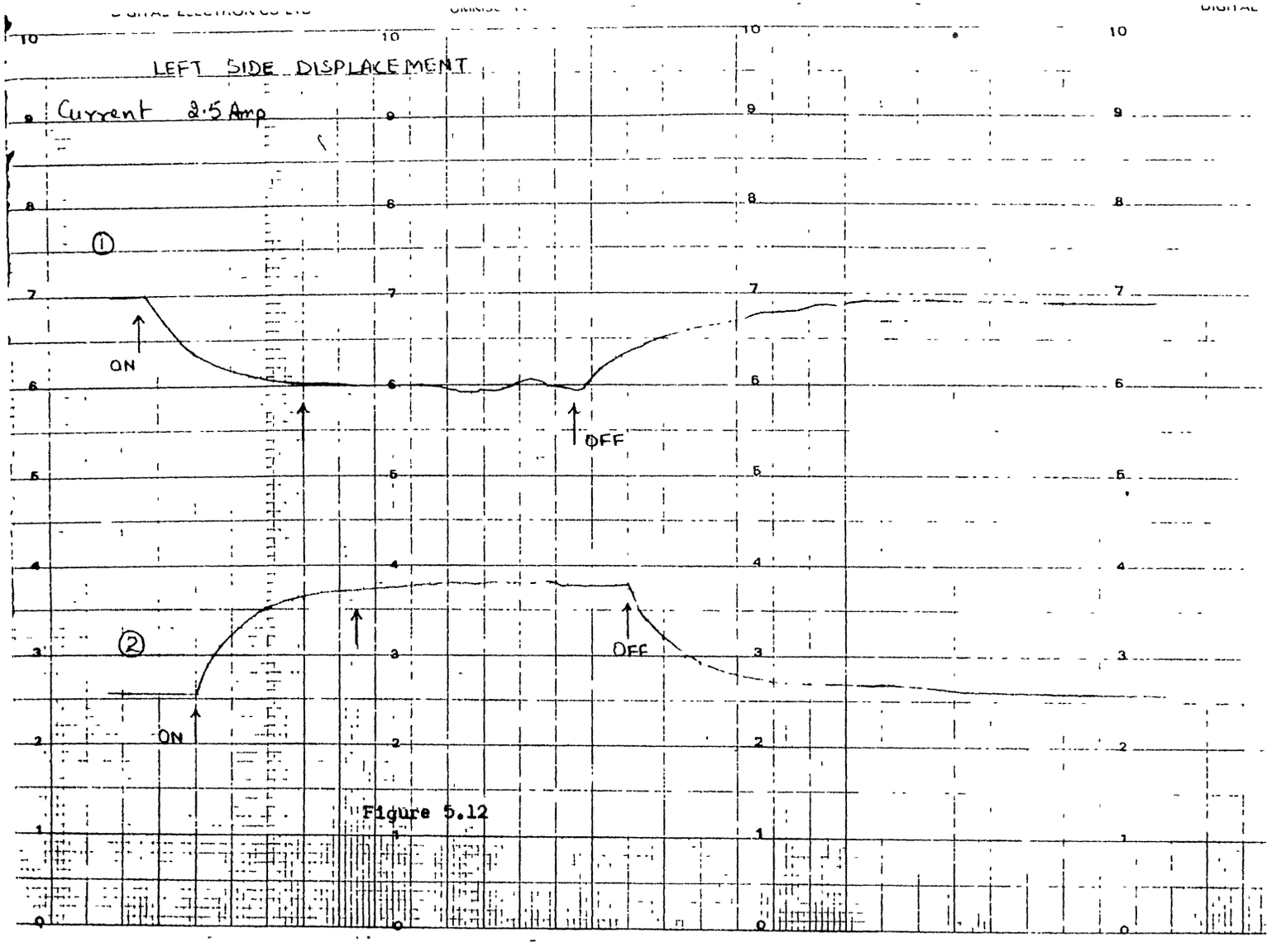

Figure 5.12

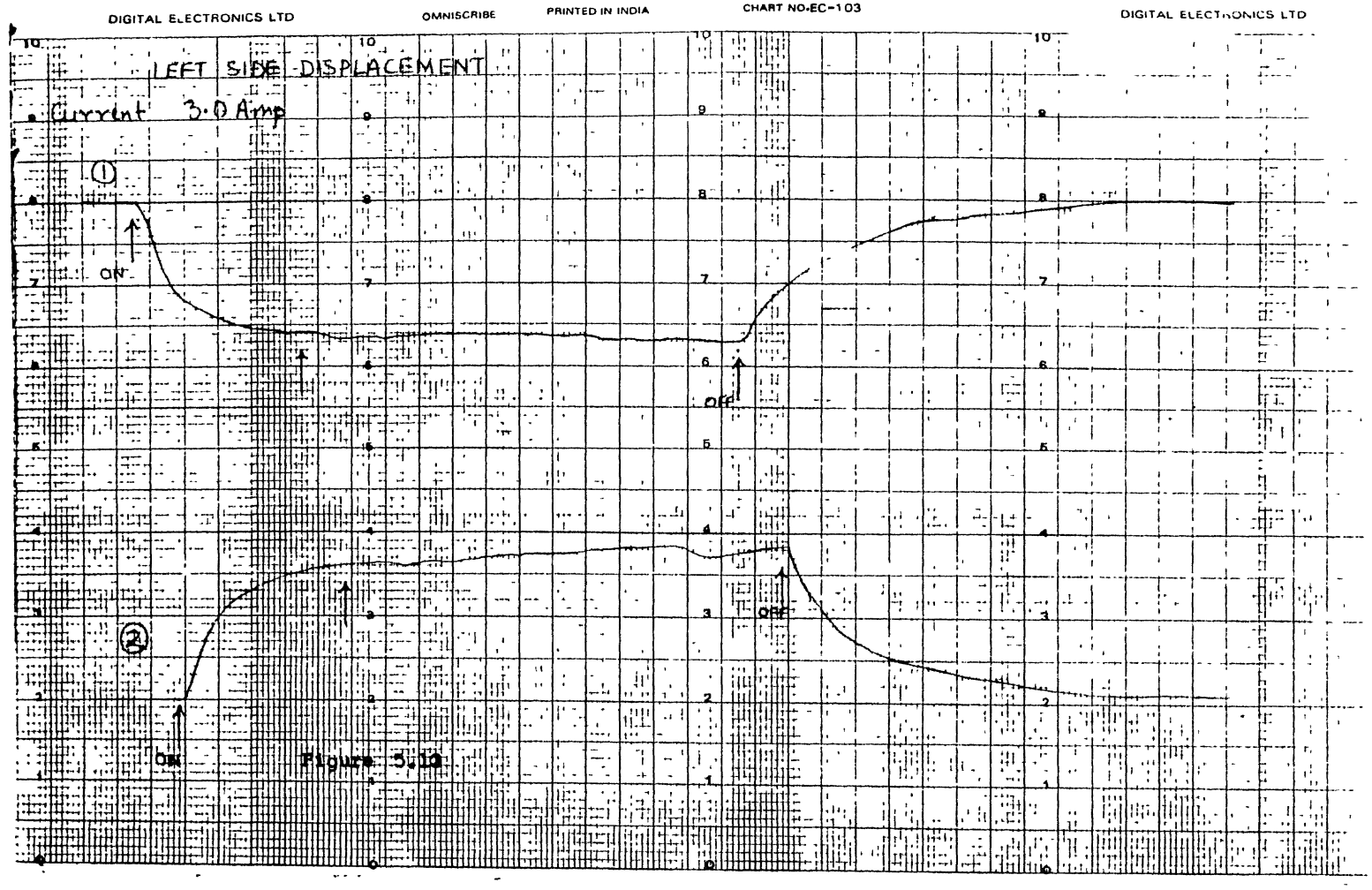
DIGITAL ELECTRONICS LTD
OMNISCRIBE
PRINTED IN INDIA
CHART NO-EC-103
DIGITAL ELECTRONICS LTD
LEFT SIDE DISPLACEMENT
Current 3.0 Amp
①
ON
②
ON
OFF
OFF

Figure 5.12

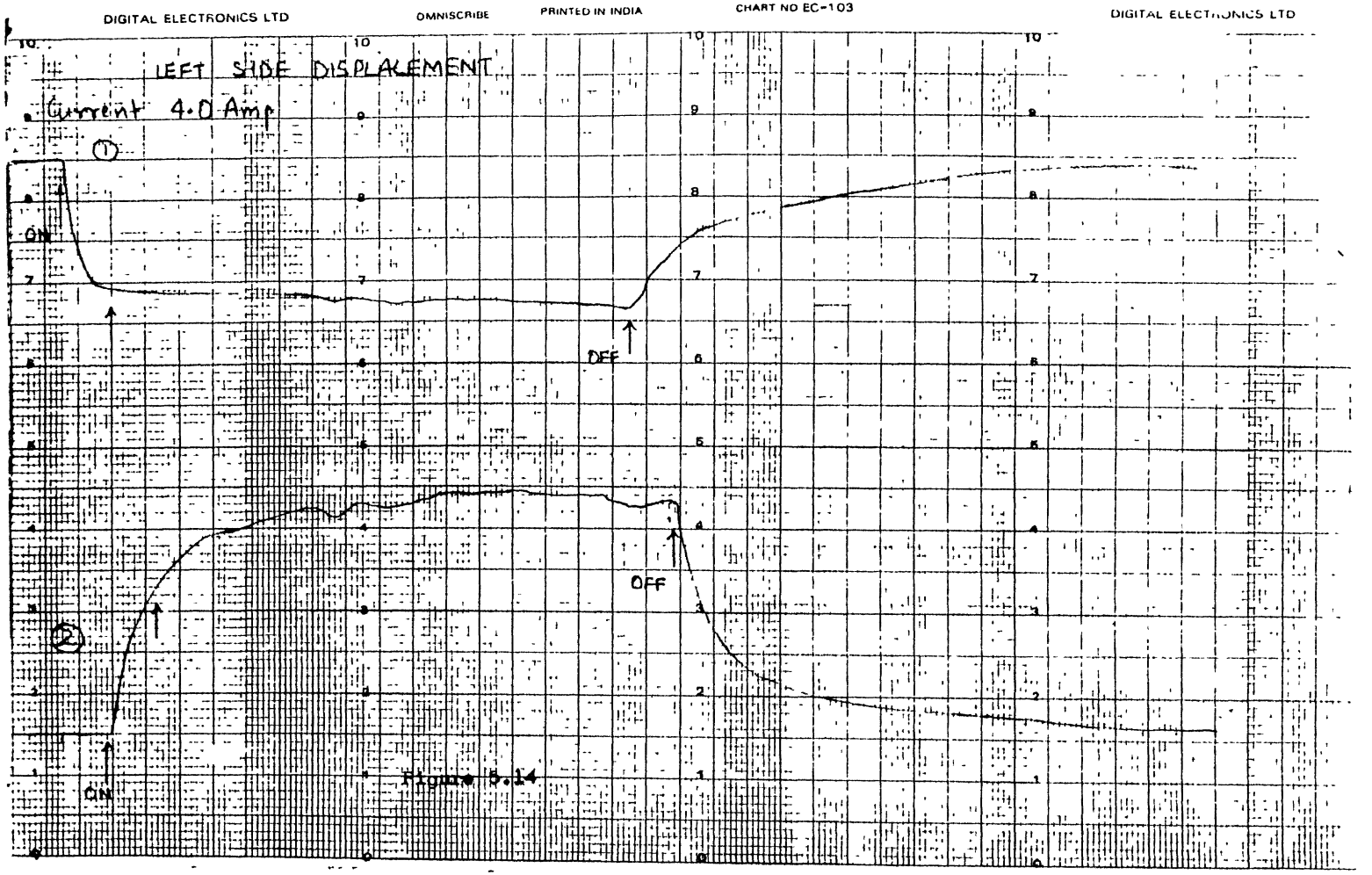
DIGITAL ELECTRONICS LTD
OMNISCRIBE
PRINTED IN INDIA
CHART NO EC-103
DIGITAL ELECTRONICS LTD
LEFT SIDE DISPLACEMENT
Current 4.0 Amp
①
ON
OFF
②
ON
OFF

Figure 5.14

TABLE 5.2

CURRENT (Amp)	MAXIMUM THERMOCOUPLE READING (mV) w.r.t air temperature L \ R	MAXIMUM TEMP (C) L\R	MAX STRAIN BRIDGE OUTPUT (mV)	MAX STRAIN (mm/mm)	DISP OBSVD (mm)	THERMPL OUTPUT AT MAX STRAIN (mV)	TEMP WHEN MAX STRAIN ACHEVD	TIME TC REACH MAX STRAIN (sec)
1.75	0.7 \0.6	42\40	0.3\0.6	0.03\0.06	0.5\1.0	0.7\0.5	42\37	173\168
2.5	1.25 \1.0	55\50	1.0\1.3	0.1 \0.13	1.3\2.4	1.2\0.7	54\42	103\103
3.0	1.8 \1.7	69\66.5	1.7\1.7	0.17\0.17	1.7\3.2	1.6\1.1	64\52	120\103
4.0	2.9 \2.4	95\85	1.8\1.8	0.18\0.18	1.8\3.2	1.7\1.2	66\54	31\31

The endpoint of the link moved by an order of 3mm which is due to the SMA wire fixed on both sides of the link. When one SMA wire contracted on heating, the other wire had to be elongated.The force required in the elongation increases with further straining after the prestrain value to about the same order as received on heating the wire. Some force was required in bending the link. The resultant force available gives the displacement.

Fixing wires on both sides of the link is a necessary evil.It can be explained i.e. if the wire is fixed on one side only then on heating, the prestrained wire reaches its contracted shape giving a large displacement of about 20 mm. But, there is no way other than the reverse bending moment of the link to bring the link back to its original position.Even though the link moves back but it cannot reach the original position because as the curvature of the link increases the force applied on the wire decreases.

5.5 DISPLACEMENT VS CURRENT FOR A COMPOSITE LINK WITH NITINOL WIRE AT 3% AND 4% PRESTRAIN

This experiment was done to find the effect of the link material and the effect of different values of prestrain in SMA wire to the displacement of the free end of the link.

The experiment showed that with composite as link material more displacement was observed as shown in figure 5.15,5.16 .This can be attributed to the decrease in the distance between SMA wire and link axis as the modulus of rigidity (EI) of this link was more than that of the steel link.Thus, the change in link material does not affect the link bending.

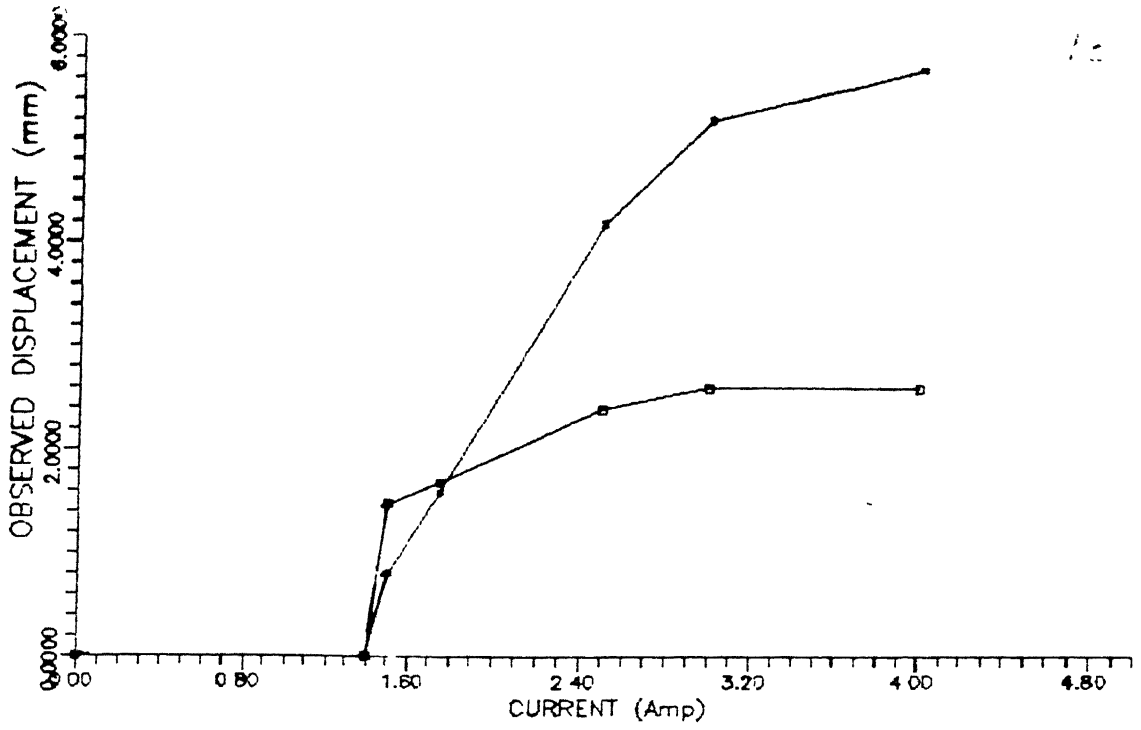

Figure5.15 Characteristics of composite link with SMA wire at 3% prestrain.

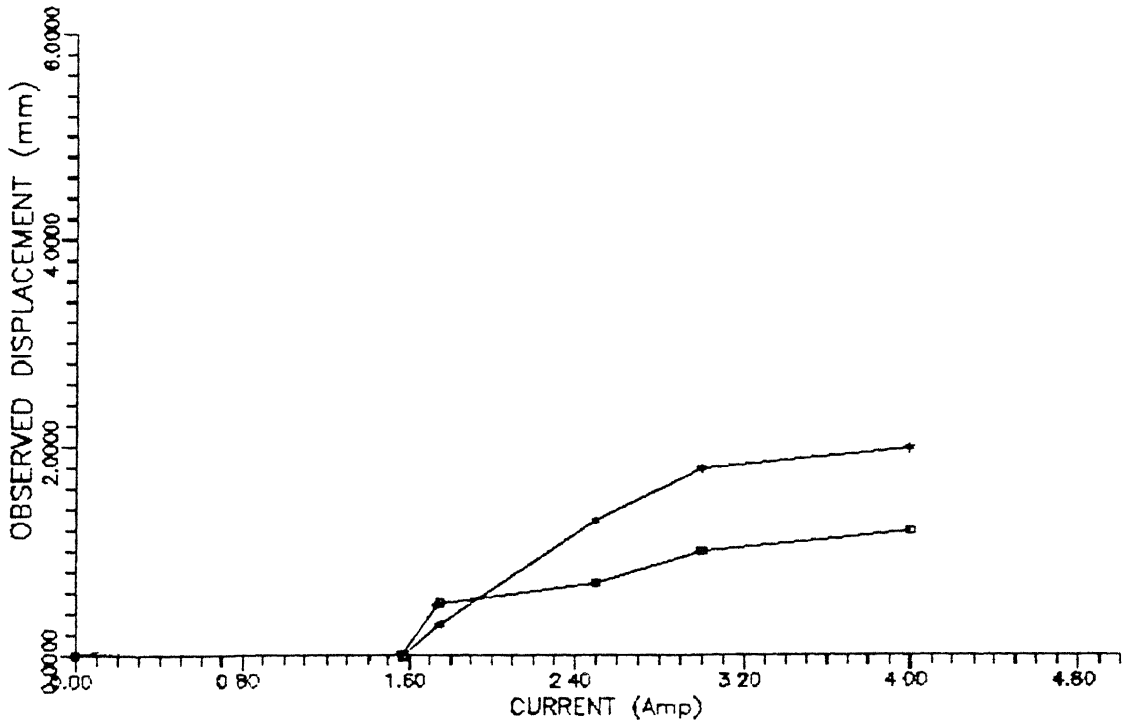

Figure 5.16 Characteristics of composite link with SMA wire at 4% prestrain

For prestrain of 3% a dead load of 17 kg was required and for 4% strain a load of 20 kg was required.Thus for increased straining more forces are required.

There was a considerable decrease in the amount of displacements observed with increased prestrain from 3% to 4% . This was due to more resistance offered by the wire which has to be elongated further on bendingof the link.

5.6 DISPLACEMENT VS CURRENT FOR A COMPOSITE LINK WITH BIOMETAL WIRE AS ACTUATOR

In this case as was stated earlier Biometal wire has reversible SME.For this link it was observed that for increasing currents the amount of displacements of the free link end increases. The maximum permissible current for this wire was 0.45 amp as max wattage was 0.8watts and the resistance of the wire was 4Ω.

The endpoint of the composite link has a maximum displacement of 40mm as shown in figure 5.17. This was due to the low modulus of rigidity of the link and the other equally important fact was that the wire was fixed on one side.This was done as biometal on cooling will regain its original (cold)position .In SMA wire this is not possible thus the other side wire was fixed to bring the link back and rotate it towards the other side. With this arrangement considerable reduction in the force acting on the actuating wire is possible with large displacements.

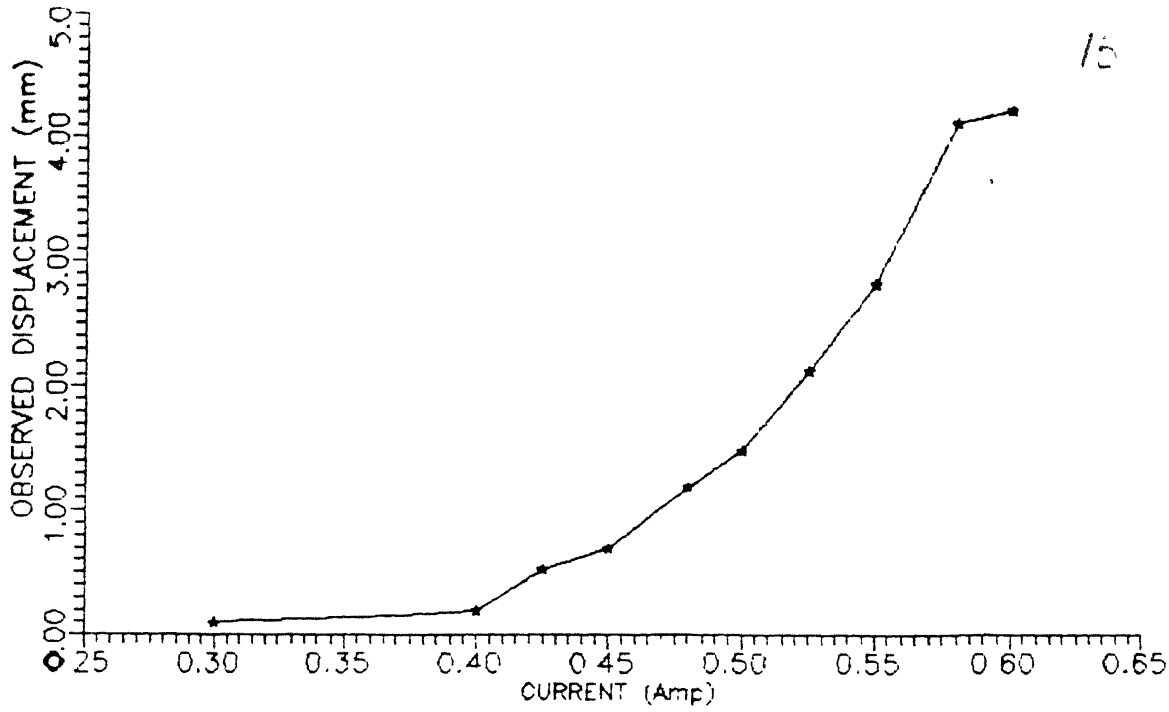

Figure 5.17 Characteristics of composite link with Biometal as actuator

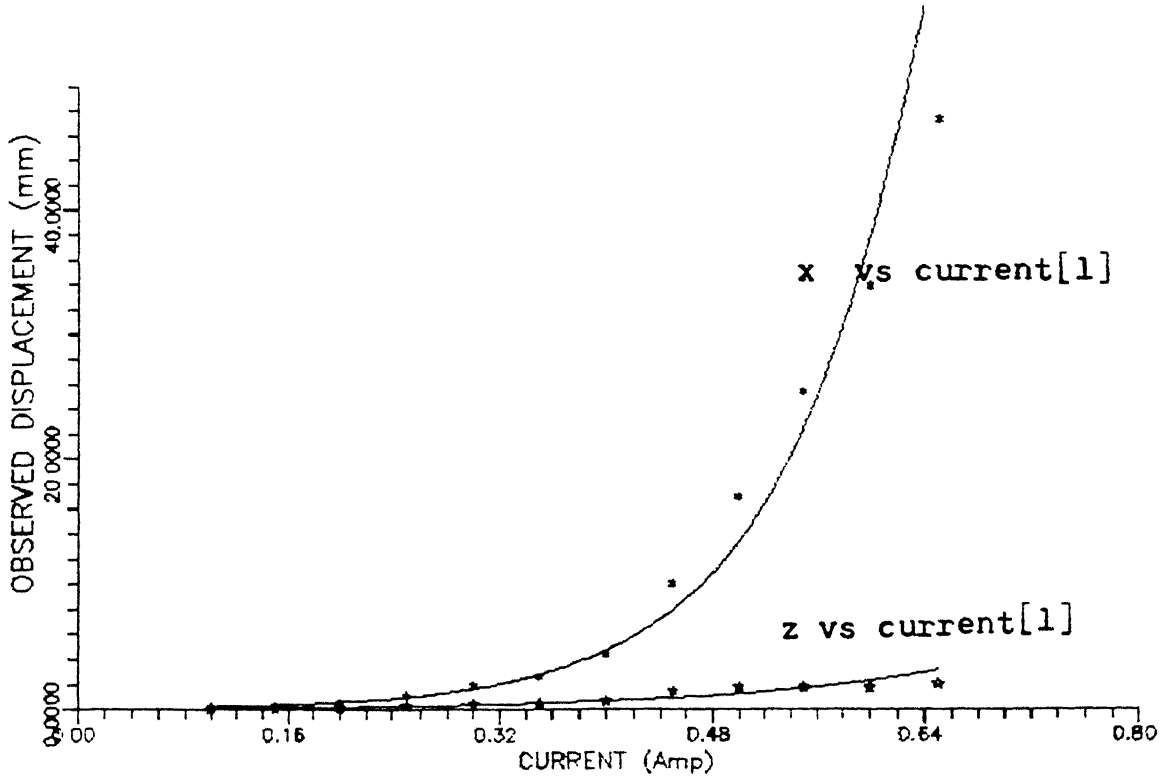

Figure 5.18 End effector displacement for varying current in Link 1.

$x = e(10.442007 \times current[1]) \times 0.072075$

$z = e(6.16393 \times current[1]) \times 0.057788$

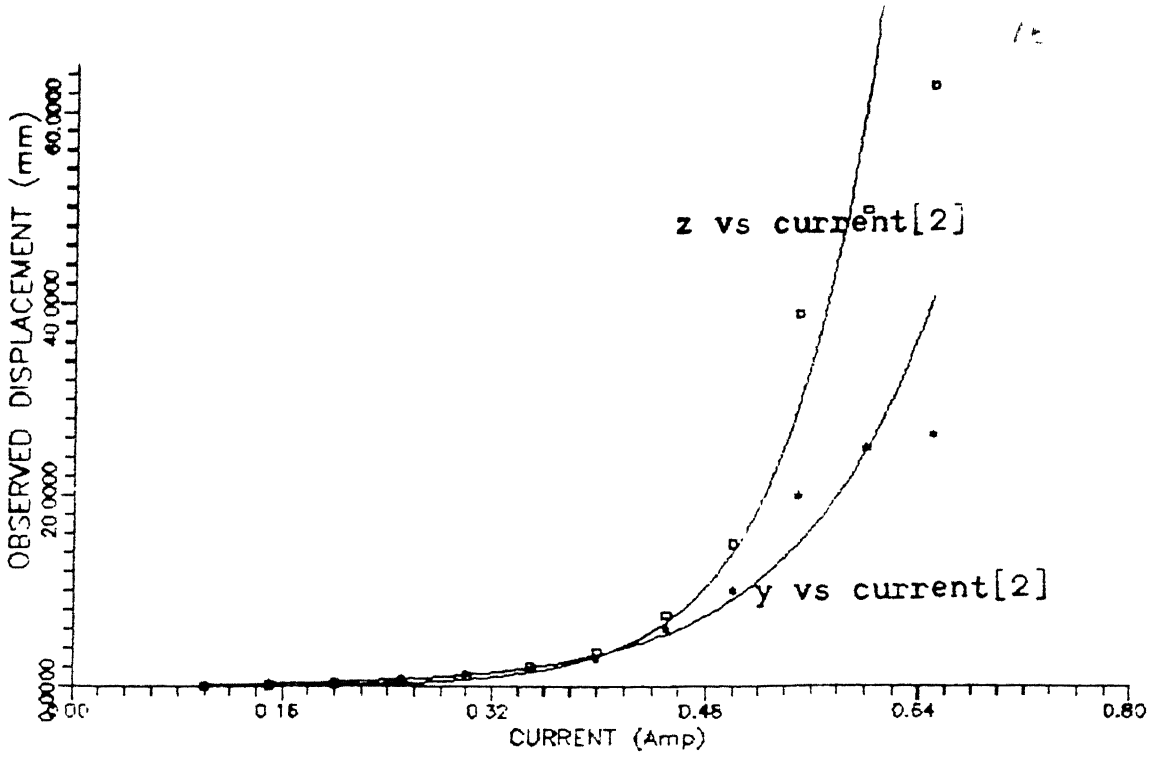

Figure 5.19 End effector displacement for varying current in Link 2.

$$y = e(14.864666 \times current[2]) \times 0.008302$$
$$z = e(10.073069 \times current[2]) \times 0.058986$$

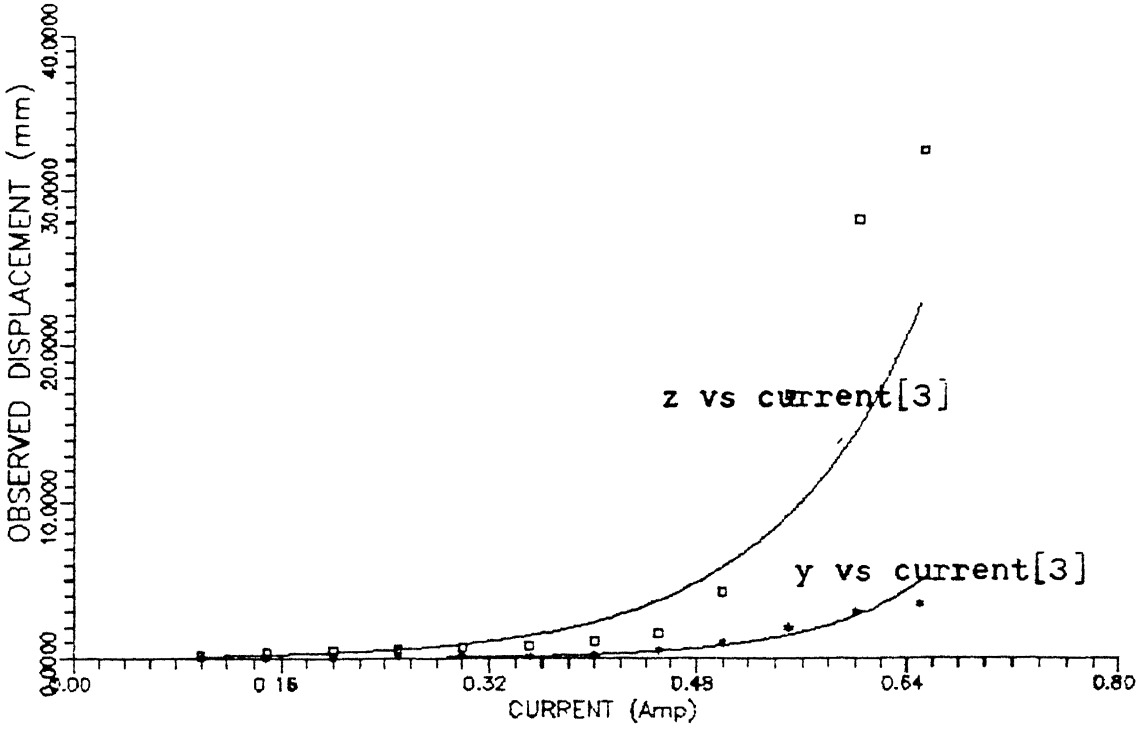

Figure 5.20 End effector displacement for varying current in Link 3.

$$z = e(14.003742 \times current[3]) \times 0.00507$$
$$y = -e(11.880694 \times current[3]) \times 0.002198$$

5.7 THREE LINK ARM OF STEEL LINKS WITH NITINOL WIRE AS ACTUATOR

An arm with three links was fabricated using spring steel plate. The configuration of this was as selected earlier. The amount of displacement for the gripper by actuation of different links was observed to be about 10mm. It had been explained earlier as to why the movement of the free end of the link was less.Thus, an arm with biometal wire was the right choice.

5.8 THREE LINK ARM OF COMPOSITE LINKS WITH BIOMETAL WIRE AS ACTUATOR

An arm of composite links actuated by the biometal wire gave a large work volume which is the foremost requirement.Some tests were conducted on this arm which are described below.

Tests were conducted for displacement achieved vs current supplied to the actuating wire. The current was firstly varied in link1 with the other two links without any supply of current as shown in figure 5.18 .Then the link2 was alone actuated (see figure 5.19) and then the link3 was only actuated (see figure 5.20).In each case the displacement of the free end of the arm was observed by a travelling microscope.Refer figure 3.3.

Next set of readings were taken with different amounts of currents being supplied to the three different links.This data is matched with the data produced from the inverse kinematic solution.

5.9 GRIPPER ACTUATION BY BIOMETAL WIRE

It was observed that the gripper jaws opened by 30 mm when there was no bias force acting on the biometal wire. When the bias force in the form of spring was placed the gripper opening

Table 5.3

Input position (x,y,z) (in mm)	Linearly interpolated current (Amp) (c1,c2,c3)	Observed position (x,y,z) (in mm)
(5,5,5)	(0.41,0.40,0.00)	(3.5,4.1,5.1)
(5,10,15)	(0.41,0.50,0.00)	(4.8,9.9,14.7)
(10,15,40)	(0.45,0.52,0.00)	(9.2,18.1,41)
(20,25,70)	(0.52,0.60,0.56)	(18.8,26.3,73.3)
(30,20,75)	(0.58,0.55,0.58)	(26.8,18.9,77.3)
(35,20,100)	(0.59,0.55,0.65)	(32.6,19.2,110)
(20,15,35)	(0.53,0.53,0.63)	(18.7,18.8,36.8)

Table 5.4

Initial position (x,y,z) (in mm)	Final position (x,y,z) (in mm)
(0.0,0.0,0.0)	(+0.0,0.0,0.0)
(0,+0.3,-0.2)	(+1.8,-1.5,+2.2)
(-0.5,+0.1,-0.2)	(+1.6,-1.5,+2.2)
(0.0,0.0,-0.3)	(+2.2,-2.0,+2.2)
(0.0,0.0,-0.2)	(-1.3,-0.5,-0.5)
(0.0,0.0,+0.2)	(+2.1,-0.5,+1.7)
(-0.3,-0.4,+0.1)	(+2.4,-1.0,+2.7)
(0.0,0.0,0.0)	(+2.7,0.0,+3.7)
(-0.5,0.0,0.0)	(0.0,-1.0,+1.4)
(0.0,0.0,-0.1)	(-0.1,-0.7,+1.7)
(0.0,0.0,0.0)	(-0.1,-1.2,+1.9)
(-0.4,0.0,+0.2)	(-0.3,-1.3,+2.1)
(-0.7,-0.4,+0.2)	(-0.4,-0.6,+2.3)
(-0.4,0.0,+0.1)	(-0.2,-0.7,+3.1)
(-0.2,-0.1,+0.1)	(-1.0,-0.7,+3.0)
(-0.2,-0.1,+0.1)	(-1.3,0.0,+1.6)
(0.0,-0.2,+0.1)	(+0.6,-0.1,+1.8)
(0.0,-0.2,+0.1)	(+0.9,-1.1,+1.8)
(-0.7,-0.2,+0.2)	(-0.3,-1.3,+1.8)
(0.1,-0.9,+1.5)	(1.0,-0.8,+1.5)

decreased to 18 mm. The spring force is used to grip the object while the biometal is required to open the jaws of the gripper.

5.10 ACCURACY AND REPEATABILITY OF THE BIOMETAL WIRE ACTUATED ARM

To find the accuracy of the presently developed arm, a test was conducted. In this test the PC was interactively given a position and the position reached by the robot arm checked by use of two travelling microscopes. The two travelling microscopes were kept perpendicularly to each other so that x,y,z coordinates of the end point could be noted. Table 3 given the input position, the linearly interpolated current between any two consecutive points known in figure 5.18, 5.19, 5.20 and the actual position reached. It can be seen that the arm is satisfactorily accurate in reaching the required position.

To test the repeatability of the arm the PC was interactively given a position to be reached and the actual position reached was noted. Then the arm was brought back to original position. Again same input was given and the actual position of the end point of the arm noted. This method was adopted for a few values given in table 4.

From the experimental results it can be stated that as the deviation from the position are not enormous the repeatability of the arm is satisfactory.

CHAPTER 6

CONCLUSION AND SCOPE FOR FUTURE WORK

6.1 CONCLUSION

A three link arm is developed using Shape Memory Alloy wires for its actuation. This arm can move from one position to another and back,repeatedly.

This arm is controlled by a Personal Computer using a digital output card with the necessary electrical interface.

The steel link with Nitinol wire gave lesser displacement than composite link. This was due to lesser distance in fixing the wire in case of composite link.

The amount of displacement of link end point decreased with increase in prestraining of Nitinol wire from 3% to 4%.

The Biometal wire actuated robot arm is light,low cost gives large displacement but has low weight carrying capacity.

The Biometal wire actuated gripper also has low weight carrying capacity.

The Biometal arm did not give good accuracy and repeatability due to control by digital pulses from the PC. Analog control should have been used.

6.2 SCOPE FOR FUTURE WORK

The control of current was by digital pulses so the arm end point keeps vibrating, thus the electrical control circuit should be based on analog control.

More Biometal wires can be fitted to the existing arm so that its load carrying capacity is increased.

More Biometal wires can be fitted to the gripper so that its load carrying capacity is increased.

REFERENCES

1) R.J. Waslewski, **"The shape memory effect in TiNi : One aspect of stress-assisted martensitic transformation"**, Edit by J.Perkins, Pelnum Press, New York, 1975, p245-271.

2) C.Rodriguez and L.C.Brown, **"The mechanical properties of SME alloys"**, Edit by J.Perkins, Pelnum Press, New York, 1975, p29-57.

3) J.Perkins, G.R. Edwards, C.R.Such, J.M.Johnson and R.R.Allen, **"Thermomechanical characteristics of alloys exhibiting martensitic thermoelasticity"**, Edit by J.Perkins, Pelnum Press, New York, 1975, p273-303.

4) W.S.Owen, **"Shape memory effects and application : An overview"**, Edit by J.Perkins, Pelnum Press, New York, 1975, p305-325.

5) **Specification sheet for Nitinol shape memory alloy**, copyright 1986, TiNi Alloy Company, U.S.A.

6) **Specification sheet for Biometal shape memory alloy**, copyright 1986, TiNi Alloy Company, U.S.A.

7) **Specification sheet for Nitinol**, copyright Innovative Technology International, Inc, U.S.A.

8) L.M.Schetky, **"Shape-memory alloys"**,

9) **Biometal Fibre: An introduction**, copyright 1986, TiNi Alloy Company, U.S.A.

10) **"Metallurgy: Extraordinary alloys that remember their past"**, Science vol191, March 1976, p934-936.

11) C.Robinson, **"shape memory alloys find expanding applications"**, Intech V34, n3, March 1987, p55-58.

APPENDIX A

The specification of NiTinol SMA wire as supplied by the TiNi Alloy company, U.S.A. are described as under :

PHYSICAL PROPERTIES OF NITINOL WIRE

Melting temperature = 1240 to 1310 C

Annealing temperature = 520 to 600 C

Density = 6.45 gram per cc

Thermal conductivity = 0.1 w/cm-deg.C

Specific heat Cp =0.211 cal/C-gm

Latent heat = 307 cal/gm

Coefficient of thermal expansion = 11E-6 /C (Austenite)
6.6E-6 /C (Martensite)

Electrical resistivity = 60$\mu\Omega$-cm (Austenite)
75$\mu\Omega$-cm (Martensite)

Young's Modulus = 700 Kbar

Yield strength = 30 Ksi

Poisson's ratio = 0.3

Hardness = 80 (Rb)

APPENDIX B

The physical properties of E- Glass Epoxy are given as under.

E = 21500 N/mm^2 (modulus of elasticity)

σ = 570 N/mm^2 (tensile strength)

ρ = 1.97 gm/cm^3 (density)

V_f = 57% (fibre volume fraction)

APPENDIX C

Geometrical data(mm)	Steel link	Composite link (A)	Composite link (B)
Length	150	150	110
Breadth	14.5	30	12
Thickness	0.55	1.2	0.5
Distance between wire & link plane	4.0	3.0	1.0

APPENDIX D

The components used in manufacturing a gripper with their sizes and materials is specified as under:

COMPONENT	SIZE	MATERIAL
1) Gripper base	50 X 40 X 1	Aluminum
2) Jaw	53 X 40 X 3	Perspex
3) Pulley	10 X 4 X 10	Bakelite
4) Biometal wire	9.05 X 0.15	TiNi
5) spring	(not specified)	spring steel